Land Processes Can Substantially Impact the Mean Climate State

Claire M. Zarakas[1], **Daniel Kennedy**[3], **Katherine Dagon**[3], **David M. Lawrence**[3], **Amy Liu**[1], **Gordon Bonan**[3], **Charles Koven**[4], **Danica Lombardozzi**[3], **and Abigail L. S. Swann**[1,2]

[1]University of Washington, Department of Atmospheric Sciences
[2]University of Washington, Department of Biology
[3]National Center for Atmospheric Research
[4]Lawrence Berkeley National Laboratory

Key Points:

- Assumptions about land processes substantially impact mean state terrestrial temperature and precipitation.
- Land parameters influence climate predominantly through changing evapotranspiration rather than through other mechanisms.
- Warming driven by land processes activates different atmospheric feedbacks than radiatively-driven warming.

Corresponding author: Claire M. Zarakas, czarakas@uw.edu

Abstract

Terrestrial processes influence the atmosphere by controlling land-to-atmosphere fluxes of energy, water, and carbon. Prior research has demonstrated that parameter uncertainty drives uncertainty in land surface fluxes. However, the influence of land process uncertainty on the climate system remains underexplored. Here, we quantify how assumptions about land processes impact climate using a perturbed parameter ensemble for 18 land parameters in the Community Earth System Model (CESM2) under preindustrial conditions. We find that an observationally-informed range of land parameters generate biogeophysical feedbacks that significantly influence the mean climate state, largely by modifying evapotranspiration. Global mean land surface temperature ranges by 2.2°C across our ensemble ($\sigma = 0.5$°C) and precipitation changes were significant and spatially variable. Our analysis demonstrates that the impacts of land parameter uncertainty on surface fluxes propagates to the entire Earth system, and provides insights into where and how land process uncertainty influences climate.

Plain Language Summary

Land processes can affect climate by controlling the transfer of energy and water from the land to the atmosphere. Previous research has shown that uncertainty surrounding land processes (e.g. photosynthesis and the movement of water through soils) can drive uncertainty in land-to-atmosphere fluxes. However, it remains unclear how much that land uncertainty can impact climate. Here, we quantify how climate is sensitive to assumptions about land processes by varying 18 land model parameters to create an ensemble of 36 possible worlds in a global climate model. Land temperature ranges by 2.2°C across this ensemble, mostly due to changes in how much water is evaporated from the land surface. Changing land parameters also drives regionally variable changes in mean precipitation. This study highlights a large and underappreciated impact of land processes in determining the mean climate state, and provides insights into how climate is influenced by land process uncertainty.

1 Introduction

Land models were initially developed to support weather and climate prediction by providing atmospheric models with lower boundary conditions of energy, water, and momentum fluxes. Given this limited scope, early land models were simple biogeophysical models, in which land-to-atmosphere fluxes were determined by prescribed land surface albedo, evaporative resistance, and roughness (Manabe, 1969). Since then, land models have substantially expanded in scope and complexity. Modern land models now represent biogeochemical cycling, hydrology, ecology, land use, and land management, and are used to predict how processes across these domains interact and respond to global change (Fisher & Koven, 2020). This evolution has been accompanied by an increase in the number of model parameters, many of which can influence land-to-atmosphere fluxes by altering the emergent land surface albedo, turbulent flux partitioning, and roughness.

The increasingly complex land model parameter space has driven a large body of research exploring the implications of land parameter uncertainty for land model calibration (Dagon et al., 2020), carbon and water flux uncertainty quantification (Hou et al., 2012; McNeall et al., 2023), and process understanding (Boulton et al., 2017). Earth system parametric uncertainty is often quantified through perturbed parameter ensembles (PPEs), in which multiple poorly constrained parameters are systematically varied within a single model structure. Land PPEs have demonstrated that parameter uncertainty is a major driver of uncertainty in land-to-atmosphere surface fluxes, at local (Ricciuto et al., 2018; Fisher et al., 2019), regional (Bauerle et al., 2014; Huo et al., 2019), and global scales (Dagon et al., 2020; Zaehle et al., 2005).

Most existing land parameter uncertainty studies have quantified parameters' impact in a land-only framework (Zaehle et al., 2005; Dagon et al., 2020; Ricciuto et al., 2018; Bauerle et al., 2014; Fisher et al., 2019; Dietze et al., 2014; Bauerle et al., 2014), where the atmospheric forcing is an external boundary condition and land surface fluxes do not influence the atmosphere. Only a handful of previous studies have assessed the biogeophysical (Liu et al., 2005; Fischer et al., 2011; Williams et al., 2016) or carbon cycle (Booth et al., 2012, 2017; L. R. Hawkins et al., 2019; McNeall et al., 2023) implications of land parameter uncertainty in a coupled context, or included land parameters in PPEs perturbing parameters across the Earth system (Sexton et al., 2021; Yamazaki et al., 2021). This is in part due to computing constraints. For example, in the Community Earth System Model version 2 (CESM2), a simulation with a dynamic atmosphere requires about ten times more computing time per modeled year than a land-only simulation, and coupled configurations often require more simulated years to establish a signal due to internal variability of the coupled system (Kay et al., 2015). Additionally, the prevalence of land-only analyses reflects the land modeling community's focus on how land parameter uncertainty influences terrestrial processes, rather than atmospheric processes. The biogeophysical impact of land parameter uncertainty on atmospheric processes and land-atmosphere interactions remains underexplored. Of the few studies which have assessed land parameter uncertainty in a coupled context, only one has quantified the biogeophysical impact of land parameters on climate globally (Fischer et al., 2011).

This is a problematic gap in the literature because land parameters' demonstrated influence on land surface fluxes suggests that land parameters can influence the mean climate state. It has been established for decades that changes in land surface albedo (Charney et al., 1975; Charney, 1975; Charney et al., 1977), roughness (Sud et al., 1988), and capacity to evaporate water (Shukla & Mintz, 1982) can alter temperature and precipitation on global scales. More recently, Laguë et al. (2019) used a modern Earth system model to show that atmospheric feedbacks are critical in determining how land temperatures respond to idealized land surface changes. Extensive previous work has demonstrated that changes in land cover can drive local, regional, and remote climate impacts (e.g. Pongratz et al., 2010; Swann et al., 2012; Boysen et al., 2020). Additionally, changing land model representations of terrestrial processes such as stomatal conductance and soil hydrology can influence the mean climate state (Lawrence et al., 2007) and frequency of extremes (Kala et al., 2016).

In this study, we aim to close this gap in the literature by using a coupled PPE to address the following questions: (1) to what extent can land parameters impact the mean climate state? and (2) through what mechanisms do land parameters influence climate?

2 Methods

We ran PPEs under preindustrial conditions using two configurations of CESM2 (Danabasoglu et al., 2020): a partially coupled configuration ("coupled") and an uncoupled, land only configuration ("land-only"). In both the coupled and land-only PPE, the land model (the Community Land Model version 5, CLM5; Lawrence et al., 2019) was run with prognostic leaf area. In the coupled ensemble, we ran preindustrial simulations with constant greenhouse gas concentrations using an active atmosphere (CAM6; Bogenschutz et al., 2018) and a slab ocean (Danabasoglu & Gent, 2009). Because these simulations have fixed concentrations of greenhouse gasses including CO_2, they capture the biogeophysical impacts of land parameters which is the focus of this paper, but they do not capture biogeochemical feedbacks. The land-only simulations used a custom atmospheric forcing, which was generated by CAM6 in the reference coupled simulation that used default parameters.

Our PPEs sampled 18 land parameters (Table S5), and our parameter selection was informed by the CLM5 PPE project (data and methods description are available via `https://`

`github.com/djk2120/clm5ppe`). The CLM5 PPE differs from ours in that the simulations were run in a land-only configuration forced with observationally-derived atmospheric data for present-day. Nonetheless, the one-at-a-time parameter perturbations provide insight into which parameters might be meaningful for our coupled PPE. We used two parameter selection criteria: (1) that parameters would likely have a large impact on the atmosphere, based on results from the CLM5 PPE, and (2) that parameters sampled different functional areas of the model (Text S2). The 18 parameters we selected are described in detail in Table S1 and span nine functional categories: soil hydrology, stomatal conductance and plant water use, snow, photosynthesis, boundary layer / roughness, radiation, canopy evaporation, biomass heat storage, and temperature acclimation.

For each parameter, we ran two simulations, where the parameter was perturbed to a minimum and maximum value (ensemble n = 36). We used the parameter ranges from the CLM5 PPE, which were determined by domain-area experts based on literature review and expert judgement. Because some parameters have larger ranges than others, our analysis includes both the sensitivity of the climate system to a change in a parameter combined with the uncertainty in that parameter's range. We note that this one-at-a-time sampling procedure does not account for parameter interactions, though we expect that parameter interactions may be of second-order importance based on Fischer et al. (2011) who finds that nonlinear interactions between parameters were minimal in a stationary climate.

3 Results and Discussion

3.1 Mean temperature changes

Our ensemble demonstrates that land parameters can substantially impact the mean climate state. Global mean land surface temperatures range by 2.2°C across our coupled PPE (σ = 0.5°C), and by over 3°C at some latitudes ($\sigma >$ 0.65°C above 67°N; Figure 1a). Seven out of 18 parameters generated a greater than 1°C temperature range (Figure 1b), and more than 70% of the land surface experienced statistically significant changes in annual mean temperature in 20 out of the 36 ensemble members (Figure S1). Global mean surface temperatures (including ocean) ranged by 1.1°C (σ = 0.5°C; Figure S2- S3), which is over 40% of the preindustrial absolute temperature range in CMIP6 (2.4°C, σ=0.58°C; Tett et al., 2022) and CMIP5 (E. Hawkins & Sutton, 2016). Three soil hydrology parameters - `frac_sat_soil_dsl_init`, `d_max`, and `fff` - had the largest impact on global mean temperature. Land surface temperature changes in the land-only PPE were generally much smaller than those in the coupled PPE (Figure 1), consistent with the fact that atmospheric feedbacks substantially amplify the land surface temperature response to changing land surface properties (Laguë et al., 2019).

Parameters generally impacted surface temperature with a similar spatial pattern globally. The leading mode of variability in annual mean surface temperature changes, as quantified by the first empirical orthogonal function (EOF; Lorenz, 1956), explains 78% of the variance across our coupled ensemble (Figure 2a, Figure S4) and is highly correlated with the global average mean land temperature change (Figure S6). As expected, the leading EOF in the land-only ensemble explains less of the temperature variance and has a different spatial pattern (Figure 2b), indicating that regional to global-scale atmospheric responses contribute to the consistent coupled PPE pattern of temperature change. Notably, the leading coupled PPE EOF differs from the typical pattern of radiatively driven warming (e.g. CO_2-driven warming, Figure 2c and Text S3), a pattern which is generally consistent across climate models (Proistosescu et al. 2020). This indicates that the dominant coupled spatial pattern is not only due to parameter-driven temperature changes kicking off radiative feedbacks (e.g. ice albedo feedback, water vapor feedback) which have consistent spatial fingerprints. Rather, this suggests that land

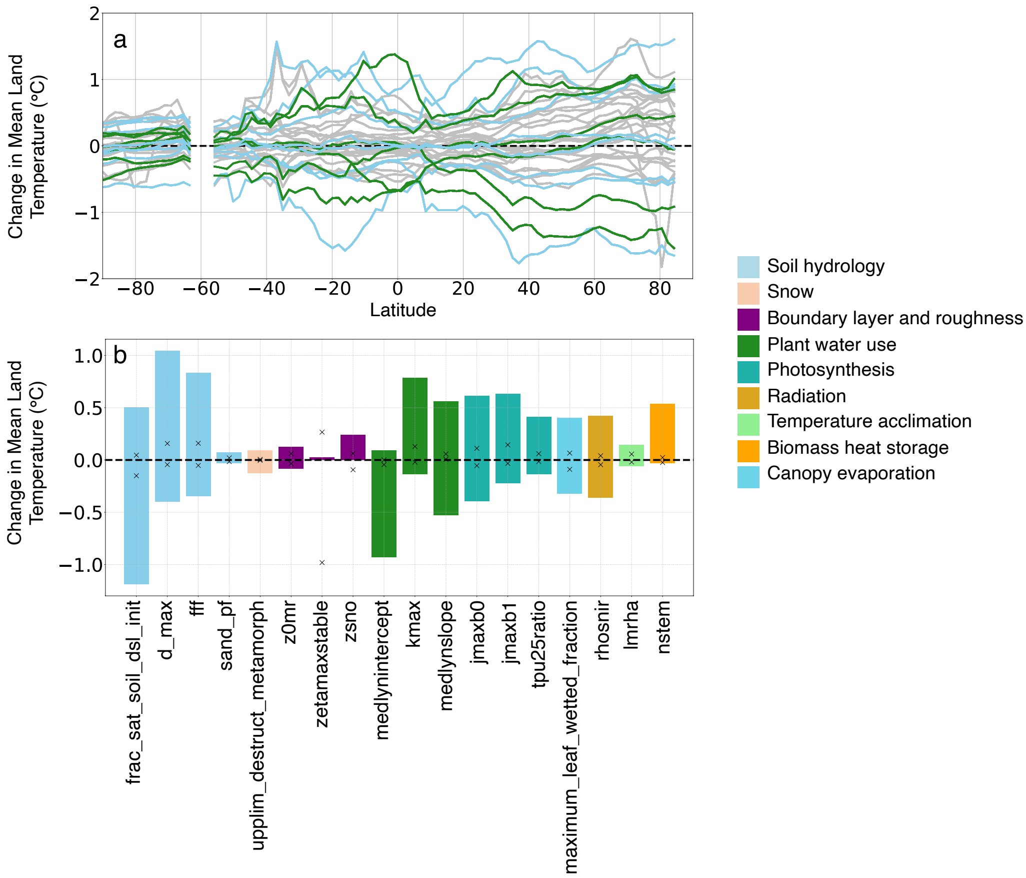

Figure 1. Zonal mean (a) and global mean (b) changes in annual land temperature across the coupled PPE, relative to the default simulation. Color indicates parameter category, and only ensemble members perturbing soil hydrology and plant water use parameters are colored in (a). In (b), bars indicate the range of coupled global mean land surface temperature changes associated with each parameter, and Xs mark the range of land-only global mean land surface temperature changes.

parameter uncertainty drives a consistent temperature response pattern, despite the fact that parameters influence different terrestrial processes.

The dominant coupled PPE temperature pattern is characterized by temperature sensitivity hotspots in the grassland ecosystems of both North America and eastern Europe / central Asia, and larger temperature changes in the Northern hemisphere than the Southern hemisphere. Across the tropics, the temperature response is larger in South America than in tropical Africa or Asia. This pattern resembles the summer temperature response to soil moisture forcing in the Global Land-Atmosphere Climate Experiment (GLACE) experiments (Koster et al., 2006; Seneviratne et al., 2013) which we discuss further in section 3.3. The hemispheric asymmetry of the land parameter temperature pattern reflects the higher land fraction in the Northern hemisphere, and land perturbations have a larger impact on climate in zonal bands with higher land fraction (Laguë et al., 2021), noting that these are for land-only zonal means and thus already take into account zonal variation in land fraction. Fischer et al. (2011)'s land PPE also generated larger land temperature changes in the Northern hemisphere than in the Southern hemisphere, but in Fischer et al. high latitude temperature changes were driven mainly by model sensitivity to snow albedo, while in our PPE most parameters drive high latitude temperature changes. Our PPE generated a larger temperature range than Fischer et al., perhaps due to the fact that Fischer et al. used a flux-corrected slab ocean which can dampen global-scale temperature responses to perturbations (Yamazaki et al., 2021).

3.2 Mean precipitation changes

We found that terrestrial precipitation is highly sensitive to land parameter choice. Global annual land mean precipitation ranged by about 5% (σ= 1%) across our ensemble, and in several regions our PPE drove annual mean precipitation changes of greater than 30% (Figure 3a). The same three soil hydrology parameters which most changed global mean temperature—`frac_sat_soil_dsl_init`, `d_max`, and `fff`—also had the largest impact on precipitation. These three hydrology parameters also generated the most extensive spatial coverage of statistically significant annual mean precipitation changes (Figure S12). Across the PPE, less of the land surface experienced statistically significant changes in annual mean precipitation compared to statistically significant changes in mean temperature (Figures S8, S10).

Changing parameters drove spatially variable signs of precipitation change, in contrast to mostly consistent signs of temperature change globally (Figure S11). Similarly, while there was a single dominant temperature response pattern across our PPE, the patterns of annual mean precipitation changes were less consistent across ensemble members. The leading EOF of precipitation change explained 48% of the variance across the PPE (Figure 3, S5) compared to the 78% temperature variance explained. This aligns with the fact that precipitation is generally more variable over time than temperature, and some of the variance across the ensemble is likely due to internal variability. Nonetheless, our PPE identified several hotspots where precipitation is the most sensitive to land parameter choice. In particular the North American Great Plains again emerged as a hotspot when considering precipitation changes on both a percentage (Figure 3) and absolute (Figure S13) basis.

Surprisingly, precipitation in the Great Plains region was not especially sensitive to land parameters in Fischer et al. (2011). However, this region has been identified as a land-atmosphere coupling hotspot due to soil moisture feedbacks in both modeling (Koster et al., 2006; Santanello et al., 2018; Zheng et al., 2015) and observational (Ferguson et al., 2012; Abdolghafoorian & Dirmeyer, 2021) studies. Many land-atmosphere studies use metrics that quantify covariances of surface fluxes and the land and atmospheric state on daily timescales. Here we are quantifying how land assumptions influence climate on decadal rather than daily timescales, but this spatial correspondence suggests that chang-

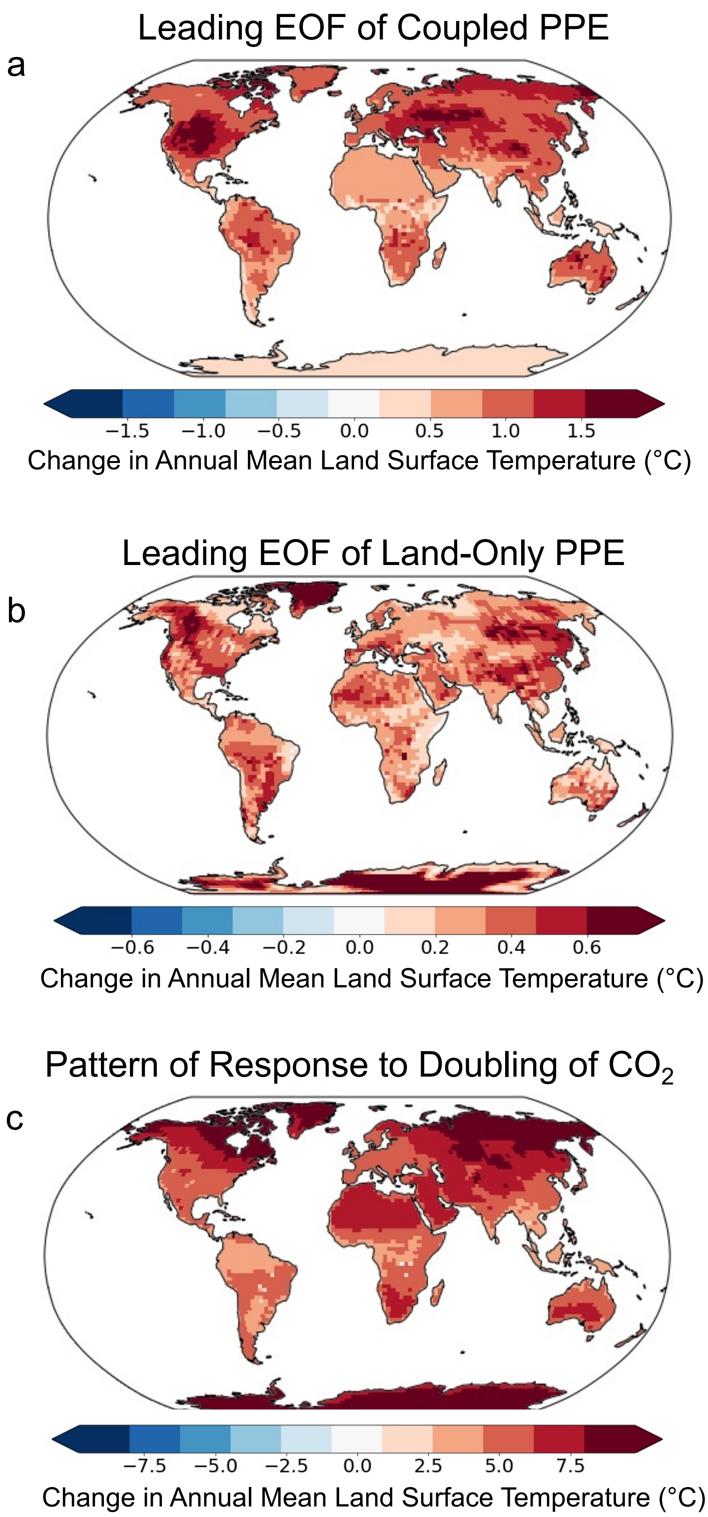

Figure 2. Spatial patterns of annual mean temperature change. The leading EOF of annual mean temperature change across (a) the coupled PPE and (b) the land-only PPE explain 78% and 65% of the variance across the coupled and land-only PPEs, respectively. The EOFs are scaled to depict two standard deviations of the variation across the ensemble along that mode of variability. The bottom panel (c) shows the CESM pattern of warming due to a doubling of CO_2 (Text S3).

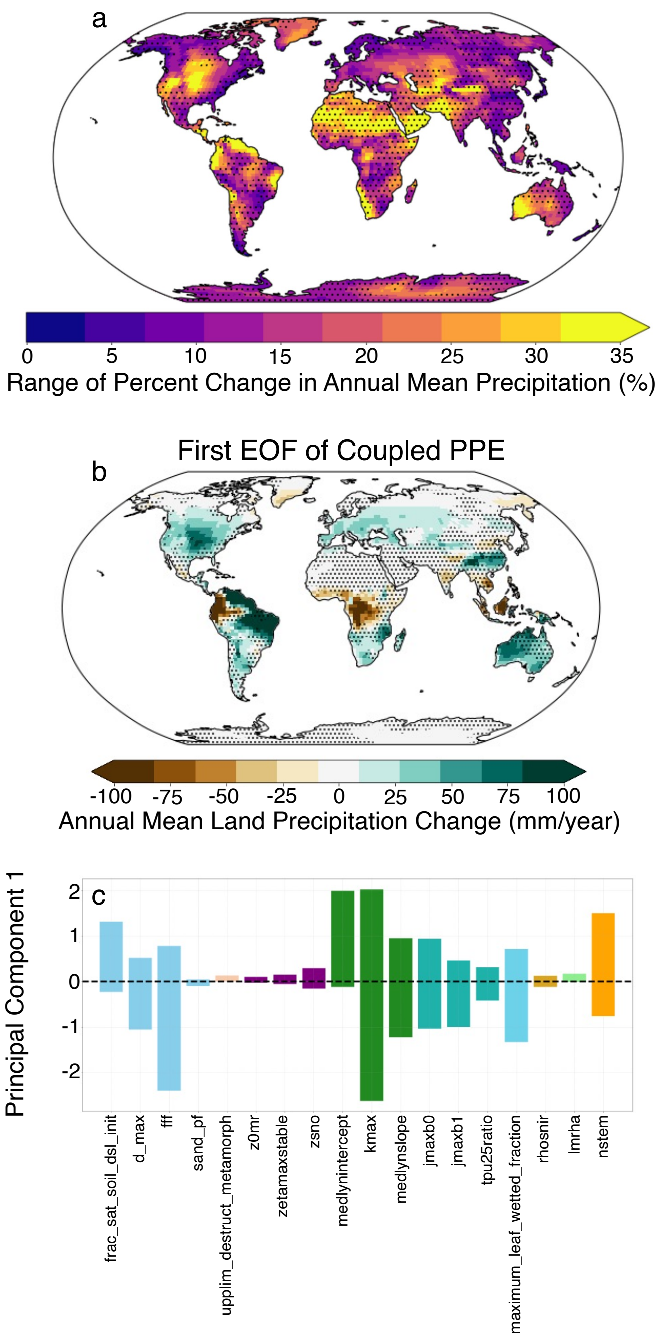

Figure 3. Range of annual mean land precipitation change across the coupled PPE. (a) Map of the range of percent changes in annual mean precipitation across the ensemble. Stippling indicates regions where precipitation changes were not statistically significant for 31 out of 36 ensemble members. (b) First EOF of precipitation changes across the coupled PPE. (c) Principal component 1 across parameters. Colors in (c) indicate parameter category as in Figure 1.

ing land parameters may influence long-term climate through mechanisms similar to the soil moisture feedbacks that drive land-atmosphere coupling on daily timescales.

3.3 Mechanisms through which land parameters influence climate

Parameters relating to soil hydrology and plant water use drove the largest temperature and precipitation changes in our ensemble (Figure 1b, 3c), highlighting that hydrological processes play a critical role in determining land temperature and precipitation. We note that we purposefully chose parameters across a range of model components and that soil hydrology parameters did not dominate the land-only CLM5 PPE rankings of parameters with the largest impact on global temperature (Figure S4), so we did not expect a priori that hydrological processes would dominate the temperature response. We also found that multiple parameters typically evaluated in the context of biogeochemical rather than biogeophysical impacts (e.g., `jmaxb0`, the baseline proportion of nitrogen allocated for electron transport; `jmaxb1` the response of the electron transport rate to light availability) can still generate large climate responses through biogeophysical pathways, consistent with prior work (Smith et al., 2017). We note that the large climate responses reflect both the climate sensitivity to a change in a parameter and the magnitude of the parameter ranges we tested. Parameters that influence boundary layer processes and roughness length drove the smallest global mean temperature changes, but they generated significant local temperature and precipitation changes, particularly over ice sheets and snow-covered regions (Figure S1).

It is challenging to fully disentangle the pathways through which parameters influence climate, because land parameters alter multiple land surface properties simultaneously. For example, increasing the parameter `kmax`, which sets the maximum plant hydraulic conductance, simultaneously changes the land surface evaporative resistance, albedo, and aerodynamic roughness, all of which influence temperature through different mechanisms. Increasing `kmax` decreases evaporative resistance by increasing the rate at which plants can transpire water, which decreases land temperatures. Increasing `kmax` also decreases plant water stress and increases leaf area, which changes albedo and thereby temperature. Increased photosynthetic rates due to reduced plant water stress also increases vegetation height, which can increase aerodynamic roughness, driving further cooling.

We used multiple linear regression to disentangle the extent to which land precipitation and temperature changes across our coupled PPE are driven by three land surface properties: albedo (α), evaporative fraction (EF), and a measure of aerodynamic coupling (r_a) (Text S4). This analysis further emphasizes that evapotranspiration changes dominate the spread in land surface temperature and precipitation responses across our PPE. Changes in evaporative fraction explained the most variance across our ensemble, with albedo playing a secondary role (Figure 4). Coupled temperature changes due to changes in aerodynamic coupling were minimal. The dominance of the evapotranspiration mechanism in our PPE may in part be due to the subset of parameters we selected from the 40 top parameters identified based on CLM5-PPE output, but nonetheless our results demonstrate that land parameters' influence on evapotranspiration is an important (and potentially the dominant) mechanism whereby which land parameters influence the mean climate state.

Further, the dominance of the evapotranspiration mechanism across our ensemble may explain why the leading EOF explains such a high percentage of temperature change variance, and why temperature and precipitation changes are correlated with each other. While we initially designed the PPE to sample multiple processes across CLM's high-dimensional parameter space (including photosynthesis, snow processes, radiation, etc.), parameters mainly impacted surface climate through changes in evapotranspiration, resulting in an ultimately low-dimensional ensemble of climate responses. We hypothesize

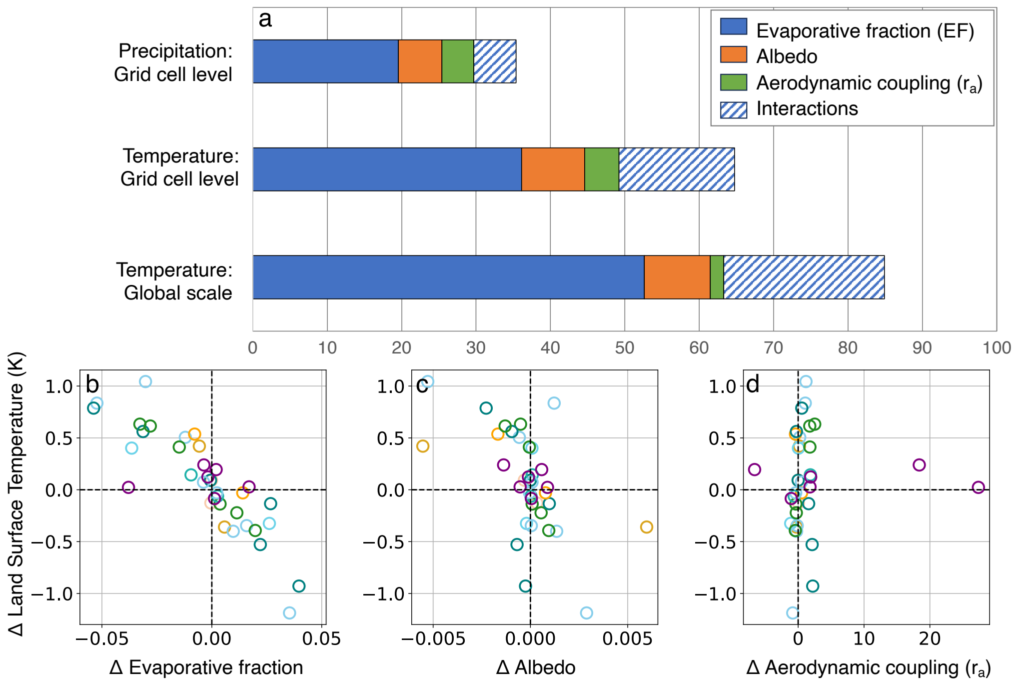

Figure 4. Relationship between land-only surface property changes and coupled land surface climate changes. The top panel (a) shows the percent variance of temperature and precipitation changes explained by each land surface property based on multiple linear regression at the grid cell level, and at the global scale for temperature. Solid colors indicate the marginal additional percentage of variance explained by each land surface property when all other predictors are included, and the hatched bar indicates the percentage variance explained by multiple predictors (i.e. the covariance between predictors). The bottom panel shows the relationships between global mean coupled land surface temperature change and land-only change in (b) evaporative fraction, (c) albedo, and (d) aerodynamic resistance across all ensemble members. Colors indicated parameter category, as in Figure 1.

that the leading EOFs of temperature and precipitation changes capture the atmospheric response to land evapotranspiration changes, which is supported by the strong correlation between land-only changes in evaporative fraction and the leading coupled temperature and precipitation EOFs (Figure S7). The spatial correspondence of mean climate changes between our PPE and GLACE experiments (Seneviratne et al., 2013) further supports this interpretation, because in GLACE experiments soil moisture forcing is also influencing climate by modifying turbulent fluxes. However, we note that the climate responses in our PPE are not directly driven by soil moisture changes. Rather, land parameter perturbations influence land evaporative resistance, which directly influences land evapotranspiration independently of any soil moisture change. That land evapotranspiration change (and associated climate feedbacks) can in turn influence soil moisture, but in our experimental design soil moisture changes are an effect or feedback, rather than an external forcing.

It has long been recognized that changes in soil moisture and evaporative resistance can impact climate (Shukla & Mintz, 1982; Sellers et al., 1996; Seneviratne et al., 2013; Laguë et al., 2019), but this is the first study to our knowledge that quantifies how parameter uncertainty associated with terrestrial controls on evapotranspiration impacts mean climate, and compares the impact of the evapotranspiration mechanism to other land surface property changes. For example, the only previous study that quantified the global biogeophysical impact of land parameter uncertainty (Fischer et al., 2011) did not evaluate the relative impact of evapotranspiration, albedo, and aerodynamic resistance changes on climate. Leveraging the results of the land-only CLM5-PPE enabled us to take a more systematic approach to parameter selection, yielding new insights which may not have emerged had we chosen parameters based on our own assumptions or prior work. This highlights the value of projects that systematically quantify and report parameter uncertainty in land models (e.g. the CLM5 PPE), which we encourage land modeling groups to incorporate as a standard part of model development and documentation efforts. This study also underscores the importance of developing better observational constraints for land parameters which influence evapotranspiration.

4 Conclusions

This study highlights a large and underappreciated impact of land processes in determining the mean climate state. We used a PPE to quantify the biogeophysical impact of land parameters on terrestrial climate. We found that land parameters can substantially impact mean temperature and precipitation, primarily through parameters' influence on evapotranspiration, and that uncertainty associated with soil hydrology and plant water use parameters drive the largest spread in the mean climate state. Uncertainty in land models' representation of land surface fluxes stems from multiple sources: internal variability, model structure, and model parameters. This study focuses on the effect of land parametric uncertainty, but our results demonstrate the importance of land process uncertainty more generally because both model structure and parameters control the land surface properties (e.g., evaporative resistance) that ultimately influence climate.

Land processes' influence on climate means that biases in land models can contribute to biases in ESM climatology. Biases in land evapotranspiration have been invoked as possible drivers for several persistent ESM biases (e.g., the central United States warm and dry summer biases, Klein et al., 2006; Cheruy et al., 2014; Williams et al., 2016; Lin et al., 2017; Morcrette et al., 2018; Zhang et al., 2018; Ma et al., 2018; Mueller & Seneviratne, 2014), and this work directly shows how land assumptions can influence the mean climate at regional and global scales, demonstrating the importance of including land perspectives in the assessments of model biases. Additionally, this study underscores that land processes primarily discussed in the context of carbon cycle uncertainty (e.g. photosynthesis) can have large biogeophysical impacts on the physical climate, in addition to their influence on atmospheric CO_2 concentration.

There has been a concerted effort across climate modeling centers to create 'digital twins' of the Earth (e.g., Voosen, 2020; Li et al., 2023) by increasing climate model resolution, thereby enabling direct modeling of fine-scale atmospheric processes such as convection that are subgrid-scale parameterizations in coarser scale models (Betancourt, 2022). While increased resolution will likely diminish biases associated with some atmospheric processes, increased resolution does less to improve land process representation because many land processes occur at molecular to hillslope scales and therefore will continue to require subgrid parameterizations (Fisher & Koven, 2020; Reichstein et al., 2019; Balaji et al., 2022). Further, finite computational resources imply tradeoffs between increasing resolution and the number of ensembles to quantify parameter uncertainty and calibrate models. If atmospheric-focused model advancements are not accompanied by efforts to improve land models, land parameter uncertainty may remain a persistent driver of climatological uncertainty and biases, even in the next generation of high-resolution climate models. Recognizing that land process uncertainty influences climate also presents an opportunity for model improvement. The climate modeling community has historically devoted more effort to atmospheric uncertainty than to land uncertainty (Hourdin et al., 2017), and we hypothesize that committing comparable resources to land parameter calibration could drive rapid improvements in model representation of present-day climate.

By demonstrating that land parameters influence the mean climate state, we hope that this study will stimulate further research into the climate impacts of land process uncertainty by a broader geophysical research community. In particular, our results suggest there is potential for land parameter uncertainty to influence the sensitivity of land temperature trends to historical and future climates, and we plan to test this in future work. Because the evaporative fraction influences how much the land surface warms in response to radiative forcing, we hypothesize that changing parameters that influence the baseline evaporative fraction will influence the modeled trajectory of land surface temperatures under increasing greenhouse gas concentrations, even if the evaporative fraction were to remain constant over time. Furthermore, land processes influence how the evaporative fraction changes over time, for example due to plant physiological responses to CO_2 (Lemordant et al., 2018). Quantifying how land parameter uncertainty influences future land temperature trajectories should be a high research priority.

While land modeling has substantially expanded beyond its initial scope of providing lower atmospheric boundary conditions into its own subdiscipline and research community, land models' continued role as atmospheric boundary conditions means that a broader climate science community must engage with land processes (and uncertainty therein) in order to understand and model the physical climate system.

5 Open Research

The model output used in this paper is available via the Dryad Digital Repository (doi:10.5061/dryad.0k6djhb73; private peer review link: `https://datadryad.org/stash/share/RGub3FTU5e5U5bLCB9bZTf96oz66ffR5DBgD3h-tGHk`). Code used to run simulations and analyze model output are available at `https://github.com/czarakas/coupled_PPE`.

Acknowledgments

CMZ was supported by the U.S. Department of Energy (DOE) Computational Science Graduate Fellowship (DE-SC0020347). The DOE Office of Biological and Environmental Research Regional and Global Model Analysis Program supported ALSS, AL, and

CMZ (DE-SC0021209); KD (DE-SC0022070); and CDK and DML (DE-AC02-05CH11231 through the RUBISCO SFA). The National Science Foundation (NSF) also supported ALSS and CMZ (AGS-1553715) and KD (NSF IA 1947282). The CESM project is supported primarily by the NSF. This material is based upon work supported by the National Center for Atmospheric Research, which is a major facility sponsored by the NSF under Cooperative Agreement No. 1852977. The Computational and Information Systems Laboratory at NCAR provided computing and data storage resources, including the Cheyenne supercomputer (https://doi.org/10.5065/D6RX99HX). We thank all scientists, software engineers, and administrators who contributed to CESM2's development.

References

Abdolghafoorian, A., & Dirmeyer, P. A. (2021, June). Validating the Land–Atmosphere Coupling Behavior in Weather and Climate Models Using Observationally Based Global Products. *Journal of Hydrometeorology*, *22*(6), 1507–1523. Retrieved 2024-01-16, from https://journals.ametsoc.org/view/journals/hydr/22/6/JHM-D-20-0183.1.xml (Publisher: American Meteorological Society Section: Journal of Hydrometeorology) doi: 10.1175/JHM-D-20-0183.1

Balaji, V., Couvreux, F., Deshayes, J., Gautrais, J., Hourdin, F., & Rio, C. (2022, November). Are general circulation models obsolete? *Proceedings of the National Academy of Sciences*, *119*(47), e2202075119. Retrieved 2023-11-13, from https://www.pnas.org/doi/10.1073/pnas.2202075119 (Publisher: Proceedings of the National Academy of Sciences) doi: 10.1073/pnas.2202075119

Bauerle, W. L., Daniels, A. B., & Barnard, D. M. (2014, May). Carbon and water flux responses to physiology by environment interactions: a sensitivity analysis of variation in climate on photosynthetic and stomatal parameters. *Climate Dynamics*, *42*(9), 2539–2554. Retrieved 2022-11-02, from https://doi.org/10.1007/s00382-013-1894-6 doi: 10.1007/s00382-013-1894-6

Betancourt, M. (2022, November). *Are We Entering The Golden Age Of Climate Modeling?* Retrieved 2023-05-30, from http://eos.org/features/are-we-entering-the-golden-age-of-climate-modeling

Bogenschutz, P. A., Gettelman, A., Hannay, C., Larson, V. E., Neale, R. B., Craig, C., & Chen, C.-C. (2018, January). The path to CAM6: coupled simulations with CAM5.4 and CAM5.5. *Geoscientific Model Development*, *11*(1), 235–255. Retrieved 2023-06-10, from https://gmd.copernicus.org/articles/11/235/2018/ (Publisher: Copernicus GmbH) doi: 10.5194/gmd-11-235-2018

Booth, B. B. B., Harris, G. R., Murphy, J. M., House, J. I., Jones, C. D., Sexton, D., & Sitch, S. (2017, April). Narrowing the Range of Future Climate Projections Using Historical Observations of Atmospheric CO2. *Journal of Climate*, *30*(8), 3039–3053. Retrieved 2023-05-03, from https://journals.ametsoc.org/view/journals/clim/30/8/jcli-d-16-0178.1.xml (Publisher: American Meteorological Society Section: Journal of Climate) doi: 10.1175/JCLI-D-16-0178.1

Booth, B. B. B., Jones, C. D., Collins, M., Totterdell, I. J., Cox, P. M., Sitch, S., ... Lloyd, J. (2012, April). High sensitivity of future global warming to land carbon cycle processes. *Environmental Research Letters*, *7*(2), 024002. Retrieved 2023-04-03, from https://dx.doi.org/10.1088/1748-9326/7/2/024002 (Publisher: IOP Publishing) doi: 10.1088/1748-9326/7/2/024002

Boulton, C. A., Booth, B. B. B., & Good, P. (2017). Exploring uncertainty of Amazon dieback in a perturbed parameter Earth system ensemble. *Global Change Biology*, *23*(12), 5032–5044. Retrieved 2023-05-29, from https://onlinelibrary.wiley.com/doi/abs/10.1111/gcb.13733 (_eprint: https://onlinelibrary.wiley.com/doi/pdf/10.1111/gcb.13733) doi: 10.1111/gcb.13733

Boysen, L. R., Brovkin, V., Pongratz, J., Lawrence, D. M., Lawrence, P., Vuichard, N., ... Lo, M.-H. (2020, November). Global climate response to idealized deforestation in CMIP6 models. *Biogeosciences*, *17*(22), 5615–5638. Retrieved 2023-05-29, from https://bg.copernicus.org/articles/17/5615/2020/ (Publisher: Copernicus GmbH) doi: 10.5194/bg-17-5615-2020

Charney, J. G. (1975). Dynamics of deserts and drought in the Sahel. *Quarterly Journal of the Royal Meteorological Society*, *101*(428), 193–202. Retrieved 2023-02-15, from https://onlinelibrary.wiley.com/doi/abs/10.1002/qj.49710142802 (_eprint: https://onlinelibrary.wiley.com/doi/pdf/10.1002/qj.49710142802) doi: 10.1002/qj.49710142802

Charney, J. G., Quirk, W. J., Chow, S.-h., & Kornfield, J. (1977, September). A Comparative Study of the Effects of Albedo Change on Drought in Semi–Arid Regions. *Journal of the Atmospheric Sciences*, *34*(9), 1366–1385. Retrieved 2023-02-15, from https://journals.ametsoc.org/view/journals/atsc/34/9/1520-0469_1977_034_1366_acsote_2_0_co_2.xml (Publisher: American Meteorological Society Section: Journal of the Atmospheric Sciences) doi: 10.1175/1520-0469(1977)034⟨1366:ACSOTE⟩2.0.CO;2

Charney, J. G., Stone, P. H., & Quirk, W. J. (1975, February). Drought in the Sahara: A Biogeophysical Feedback Mechanism. *Science*, *187*(4175), 434–435. Retrieved 2023-02-15, from https://www.science.org/doi/10.1126/science.187.4175.434 (Publisher: American Association for the Advancement of Science) doi: 10.1126/science.187.4175.434

Cheruy, F., Dufresne, J. L., Hourdin, F., & Ducharne, A. (2014). Role of clouds and land-atmosphere coupling in midlatitude continental summer warm biases and climate change amplification in CMIP5 simulations. *Geophysical Research Letters*, *41*(18), 6493–6500. Retrieved 2023-12-28, from https://onlinelibrary.wiley.com/doi/abs/10.1002/2014GL061145 (_eprint: https://onlinelibrary.wiley.com/doi/pdf/10.1002/2014GL061145) doi: 10.1002/2014GL061145

Dagon, K., Sanderson, B. M., Fisher, R. A., & Lawrence, D. M. (2020, December). A machine learning approach to emulation and biophysical parameter estimation with the Community Land Model, version 5. *Advances in Statistical Climatology, Meteorology and Oceanography*, *6*(2), 223–244. Retrieved 2022-11-02, from https://ascmo.copernicus.org/articles/6/223/2020/ (Publisher: Copernicus GmbH) doi: 10.5194/ascmo-6-223-2020

Danabasoglu, G., & Gent, P. R. (2009, May). Equilibrium Climate Sensitivity: Is It Accurate to Use a Slab Ocean Model? *Journal of Climate*, *22*(9), 2494–2499. Retrieved 2023-11-15, from https://journals.ametsoc.org/view/journals/clim/22/9/2008jcli2596.1.xml (Publisher: American Meteorological Society Section: Journal of Climate) doi: 10.1175/2008JCLI2596.1

Danabasoglu, G., Lamarque, J.-F., Bacmeister, J., Bailey, D. A., DuVivier, A. K., Edwards, J., ... Strand, W. G. (2020, January). The Community Earth System Model version 2 (CESM2). *Journal of Advances in Modeling Earth Systems*, *n/a*(n/a). Retrieved 2020-02-01, from https://agupubs.onlinelibrary.wiley.com/doi/abs/10.1029/2019MS001916 doi: 10.1029/2019MS001916

Dietze, M. C., Serbin, S. P., Davidson, C., Desai, A. R., Feng, X., Kelly, R., ... Wang, D. (2014). A quantitative assessment of a terrestrial biosphere model's data needs across North American biomes. *Journal of Geophysical Research: Biogeosciences*, *119*(3), 286–300. Retrieved 2023-12-13, from https://onlinelibrary.wiley.com/doi/abs/10.1002/2013JG002392 (_eprint: https://onlinelibrary.wiley.com/doi/pdf/10.1002/2013JG002392) doi: 10.1002/2013JG002392

Ferguson, C. R., Wood, E. F., & Vinukollu, R. K. (2012, June). A Global Intercomparison of Modeled and Observed Land–Atmosphere Coupling. *Journal* *of Hydrometeorology*, *13*(3), 749–784. Retrieved 2024-01-16, from https://journals.ametsoc.org/view/journals/hydr/13/3/jhm-d-11-0119_1.xml (Publisher: American Meteorological Society Section: Journal of Hydrometeorology) doi: 10.1175/JHM-D-11-0119.1

Fischer, E. M., Lawrence, D. M., & Sanderson, B. M. (2011, October). Quantifying uncertainties in projections of extremes—a perturbed land surface parameter experiment. *Climate Dynamics*, *37*(7), 1381–1398. Retrieved 2022-11-02, from https://doi.org/10.1007/s00382-010-0915-y doi: 10.1007/s00382-010-0915-y

Fisher, R. A., & Koven, C. D. (2020). Perspectives on the Future of Land Surface Models and the Challenges of Representing Complex Terrestrial Systems. *Journal of Advances in Modeling Earth Systems*, *12*(4), e2018MS001453. Retrieved 2023-02-08, from https://onlinelibrary.wiley.com/doi/abs/10.1029/2018MS001453 (_eprint: https://onlinelibrary.wiley.com/doi/pdf/10.1029/2018MS001453) doi: 10.1029/2018MS001453

Fisher, R. A., Wieder, W. R., Sanderson, B. M., Koven, C. D., Oleson, K. W., Xu, C., … Lawrence, D. M. (2019). Parametric Controls on Vegetation Responses to Biogeochemical Forcing in the CLM5. *Journal of Advances in Modeling Earth Systems*. Retrieved 2020-01-23, from https://agupubs.onlinelibrary.wiley.com/doi/full/10.1029/2019MS001609 doi: 10.1029/2019MS001609

Hawkins, E., & Sutton, R. (2016, June). Connecting Climate Model Projections of Global Temperature Change with the Real World. *Bulletin of the American Meteorological Society*, *97*(6), 963–980. Retrieved 2023-06-10, from https://journals.ametsoc.org/view/journals/bams/97/6/bams-d-14-00154.1.xml (Publisher: American Meteorological Society Section: Bulletin of the American Meteorological Society) doi: 10.1175/BAMS-D-14-00154.1

Hawkins, L. R., Rupp, D. E., McNeall, D. J., Li, S., Betts, R. A., Mote, P. W., … Wallom, D. C. H. (2019). Parametric Sensitivity of Vegetation Dynamics in the TRIFFID Model and the Associated Uncertainty in Projected Climate Change Impacts on Western U.S. Forests. *Journal of Advances in Modeling Earth Systems*, *11*(8), 2787–2813. Retrieved 2022-11-02, from https://onlinelibrary.wiley.com/doi/abs/10.1029/2018MS001577 (_eprint: https://onlinelibrary.wiley.com/doi/pdf/10.1029/2018MS001577) doi: 10.1029/2018MS001577

Hou, Z., Huang, M., Leung, L. R., Lin, G., & Ricciuto, D. M. (2012). Sensitivity of surface flux simulations to hydrologic parameters based on an uncertainty quantification framework applied to the Community Land Model. *Journal of Geophysical Research: Atmospheres*, *117*(D15). Retrieved 2023-05-29, from https://onlinelibrary.wiley.com/doi/abs/10.1029/2012JD017521 (_eprint: https://onlinelibrary.wiley.com/doi/pdf/10.1029/2012JD017521) doi: 10.1029/2012JD017521

Hourdin, F., Mauritsen, T., Gettelman, A., Golaz, J.-C., Balaji, V., Duan, Q., … Williamson, D. (2017, March). The Art and Science of Climate Model Tuning. *Bulletin of the American Meteorological Society*, *98*(3), 589–602. Retrieved 2023-11-13, from https://journals.ametsoc.org/view/journals/bams/98/3/bams-d-15-00135.1.xml (Publisher: American Meteorological Society Section: Bulletin of the American Meteorological Society) doi: 10.1175/BAMS-D-15-00135.1

Huo, X., Gupta, H., Niu, G.-Y., Gong, W., & Duan, Q. (2019). Parameter Sensitivity Analysis for Computationally Intensive Spatially Distributed Dynamical Environmental Systems Models. *Journal of Advances in Modeling Earth Systems*, *11*(9), 2896–2909. Retrieved 2022-11-02, from https://onlinelibrary.wiley.com/doi/abs/10.1029/2018MS001573 (_eprint: https://onlinelibrary.wiley.com/doi/pdf/10.1029/2018MS001573) doi: 10.1029/

2018MS001573
Kala, J., De Kauwe, M. G., Pitman, A. J., Medlyn, B. E., Wang, Y.-P., Lorenz, R., & Perkins-Kirkpatrick, S. E. (2016, March). Impact of the representation of stomatal conductance on model projections of heatwave intensity. *Scientific Reports*, *6*(1), 23418. Retrieved 2020-09-09, from `https://www.nature.com/articles/srep23418` doi: 10.1038/srep23418
Kay, J. E., Deser, C., Phillips, A., Mai, A., Hannay, C., Strand, G., ... Vertenstein, M. (2015, August). The Community Earth System Model (CESM) Large Ensemble Project: A Community Resource for Studying Climate Change in the Presence of Internal Climate Variability. *Bulletin of the American Meteorological Society*, *96*(8), 1333–1349. Retrieved 2023-03-23, from `https://journals.ametsoc.org/view/journals/bams/96/8/bams-d-13-00255.1.xml` (Publisher: American Meteorological Society Section: Bulletin of the American Meteorological Society) doi: 10.1175/BAMS-D-13-00255.1
Klein, S. A., Jiang, X., Boyle, J., Malyshev, S., & Xie, S. (2006). Diagnosis of the summertime warm and dry bias over the U.S. Southern Great Plains in the GFDL climate model using a weather forecasting approach. *Geophysical Research Letters*, *33*(18). Retrieved 2023-12-28, from `https://onlinelibrary.wiley.com/doi/abs/10.1029/2006GL027567` (_eprint: https://onlinelibrary.wiley.com/doi/pdf/10.1029/2006GL027567) doi: 10.1029/2006GL027567
Koster, R. D., Sud, Y. C., Guo, Z., Dirmeyer, P. A., Bonan, G., Oleson, K. W., ... Xue, Y. (2006, August). GLACE: The Global Land–Atmosphere Coupling Experiment. Part I: Overview. *Journal of Hydrometeorology*, *7*(4), 590–610. Retrieved 2023-06-10, from `https://journals.ametsoc.org/view/journals/hydr/7/4/jhm510_1.xml` (Publisher: American Meteorological Society Section: Journal of Hydrometeorology) doi: 10.1175/JHM510.1
Laguë, M. M., Bonan, G. B., & Swann, A. L. S. (2019, September). Separating the Impact of Individual Land Surface Properties on the Terrestrial Surface Energy Budget in both the Coupled and Uncoupled Land–Atmosphere System. *Journal of Climate*, *32*(18), 5725–5744. Retrieved 2023-04-03, from `https://journals.ametsoc.org/view/journals/clim/32/18/jcli-d-18-0812.1.xml` (Publisher: American Meteorological Society Section: Journal of Climate) doi: 10.1175/JCLI-D-18-0812.1
Laguë, M. M., Pietschnig, M., Ragen, S., Smith, T. A., & Battisti, D. S. (2021, March). Terrestrial Evaporation and Global Climate: Lessons from Northland, a Planet with a Hemispheric Continent. *Journal of Climate*, *34*(6), 2253–2276. Retrieved 2023-11-15, from `https://journals.ametsoc.org/view/journals/clim/34/6/JCLI-D-20-0452.1.xml` (Publisher: American Meteorological Society Section: Journal of Climate) doi: 10.1175/JCLI-D-20-0452.1
Lawrence, D. M., Fisher, R. A., Koven, C. D., Oleson, K. W., Swenson, S. C., Bonan, G., ... Zeng, X. (2019). The Community Land Model Version 5: Description of New Features, Benchmarking, and Impact of Forcing Uncertainty. *Journal of Advances in Modeling Earth Systems*, *11*, 4245–4287. Retrieved 2019-12-28, from `https://agupubs.onlinelibrary.wiley.com/doi/abs/10.1029/2018MS001583` doi: 10.1029/2018MS001583
Lawrence, D. M., Thornton, P. E., Oleson, K. W., & Bonan, G. B. (2007, August). The Partitioning of Evapotranspiration into Transpiration, Soil Evaporation, and Canopy Evaporation in a GCM: Impacts on Land–Atmosphere Interaction. *Journal of Hydrometeorology*, *8*(4), 862–880. Retrieved 2023-02-14, from `https://journals.ametsoc.org/view/journals/hydr/8/4/jhm596_1.xml` (Publisher: American Meteorological Society Section: Journal of Hydrometeorology) doi: 10.1175/JHM596.1
Lemordant, L., Gentine, P., Swann, A. S., Cook, B. I., & Scheff, J. (2018, April). Critical impact of vegetation physiology on the continental hydrologic cycle in

response to increasing CO2. *Proceedings of the National Academy of Sciences*, *115*(16), 4093–4098. Retrieved 2023-04-03, from https://www.pnas.org/doi/abs/10.1073/pnas.1720712115 doi: 10.1073/pnas.1720712115

Li, X., Feng, M., Ran, Y., Su, Y., Liu, F., Huang, C., ... Guo, H. (2023, May). Big Data in Earth system science and progress towards a digital twin. *Nature Reviews Earth & Environment*, *4*(5), 319–332. Retrieved 2024-01-04, from https://www.nature.com/articles/s43017-023-00409-w (Number: 5 Publisher: Nature Publishing Group) doi: 10.1038/s43017-023-00409-w

Lin, Y., Dong, W., Zhang, M., Xie, Y., Xue, W., Huang, J., & Luo, Y. (2017, October). Causes of model dry and warm bias over central U.S. and impact on climate projections. *Nature Communications*, *8*(1), 881. Retrieved 2023-12-28, from https://www.nature.com/articles/s41467-017-01040-2 (Number: 1 Publisher: Nature Publishing Group) doi: 10.1038/s41467-017-01040-2

Liu, Y., Gupta, H. V., Sorooshian, S., Bastidas, L. A., & Shuttleworth, W. J. (2005, April). Constraining Land Surface and Atmospheric Parameters of a Locally Coupled Model Using Observational Data. *Journal of Hydrometeorology*, *6*(2), 156–172. Retrieved 2023-02-15, from https://journals.ametsoc.org/view/journals/hydr/6/2/jhm407_1.xml (Publisher: American Meteorological Society Section: Journal of Hydrometeorology) doi: 10.1175/JHM407.1

Lorenz, E. N. (1956, December). *Empirical Orthogonal Functions and Statistical Weather Prediction* (Scientific Report No. 1). Cambridge, MA: Massachusetts Institute of Technology, Department of Meteorology. Retrieved 2023-01-04, from https://eapsweb.mit.edu/sites/default/files/Empirical_Orthogonal_Functions_1956.pdf

Ma, H.-Y., Klein, S. A., Xie, S., Zhang, C., Tang, S., Tang, Q., ... Wang, Y.-C. (2018). CAUSES: On the Role of Surface Energy Budget Errors to the Warm Surface Air Temperature Error Over the Central United States. *Journal of Geophysical Research: Atmospheres*, *123*(5), 2888–2909. Retrieved 2023-12-28, from https://onlinelibrary.wiley.com/doi/abs/10.1002/2017JD027194 (_eprint: https://onlinelibrary.wiley.com/doi/pdf/10.1002/2017JD027194) doi: 10.1002/2017JD027194

Manabe, S. (1969, November). CLIMATE AND THE OCEAN CIRCULATION: I. THE ATMOSPHERIC CIRCULATION AND THE HYDROLOGY OF THE EARTH'S SURFACE. *Monthly Weather Review*, *97*(11), 739–774. Retrieved 2024-01-04, from https://journals.ametsoc.org/view/journals/mwre/97/11/1520-0493_1969_097_0739_catoc_2_3_co_2.xml (Publisher: American Meteorological Society Section: Monthly Weather Review) doi: 10.1175/1520-0493(1969)097⟨0739:CATOC⟩2.3.CO;2

McNeall, D., Robertson, E., & Wiltshire, A. (2023, February). Constraining the carbon cycle in JULES-ES-1.0. *Geoscientific Model Development Discussions*, 1–38. Retrieved 2023-05-29, from https://gmd.copernicus.org/preprints/gmd-2022-280/ (Publisher: Copernicus GmbH) doi: 10.5194/gmd-2022-280

Morcrette, C. J., Van Weverberg, K., Ma, H.-Y., Ahlgrimm, M., Bazile, E., Berg, L. K., ... Petch, J. (2018). Introduction to CAUSES: Description of Weather and Climate Models and Their Near-Surface Temperature Errors in 5 day Hindcasts Near the Southern Great Plains. *Journal of Geophysical Research: Atmospheres*, *123*(5), 2655–2683. Retrieved 2023-12-28, from https://onlinelibrary.wiley.com/doi/abs/10.1002/2017JD027199 (_eprint: https://onlinelibrary.wiley.com/doi/pdf/10.1002/2017JD027199) doi: 10.1002/2017JD027199

Mueller, B., & Seneviratne, S. I. (2014). Systematic land climate and evapotranspiration biases in CMIP5 simulations. *Geophysical Research Letters*, *41*(1), 128–134. Retrieved 2023-05-30, from https://onlinelibrary.wiley.com/doi/abs/10.1002/2013GL058055 (_eprint: https://onlinelibrary.wiley.com/doi/pdf/10.1002/2013GL058055) doi: 10.1002/

2013GL058055
Pongratz, J., Reick, C. H., Raddatz, T., & Claussen, M. (2010). Biogeophysical versus biogeochemical climate response to historical anthropogenic land cover change. *Geophysical Research Letters*, *37*(8). Retrieved 2023-05-29, from https://onlinelibrary.wiley.com/doi/abs/10.1029/2010GL043010 (_eprint: https://onlinelibrary.wiley.com/doi/pdf/10.1029/2010GL043010) doi: 10.1029/2010GL043010
Reichstein, M., Camps-Valls, G., Stevens, B., Jung, M., Denzler, J., Carvalhais, N., & Prabhat. (2019, February). Deep learning and process understanding for data-driven Earth system science. *Nature*, *566*(7743), 195–204. Retrieved 2023-11-12, from https://www.nature.com/articles/s41586-019-0912-1 (Number: 7743 Publisher: Nature Publishing Group) doi: 10.1038/s41586-019-0912-1
Ricciuto, D., Sargsyan, K., & Thornton, P. (2018). The Impact of Parametric Uncertainties on Biogeochemistry in the E3SM Land Model. *Journal of Advances in Modeling Earth Systems*, *10*(2), 297–319. Retrieved 2022-11-02, from https://onlinelibrary.wiley.com/doi/abs/10.1002/2017MS000962 (_eprint: https://onlinelibrary.wiley.com/doi/pdf/10.1002/2017MS000962) doi: 10.1002/2017MS000962
Santanello, J. A., Dirmeyer, P. A., Ferguson, C. R., Findell, K. L., Tawfik, A. B., Berg, A., ... Wulfmeyer, V. (2018, June). Land–Atmosphere Interactions: The LoCo Perspective. *Bulletin of the American Meteorological Society*, *99*(6), 1253–1272. Retrieved 2023-11-14, from https://journals.ametsoc.org/view/journals/bams/99/6/bams-d-17-0001.1.xml (Publisher: American Meteorological Society Section: Bulletin of the American Meteorological Society) doi: 10.1175/BAMS-D-17-0001.1
Sellers, P. J., Bounoua, L., Collatz, G. J., Randall, D. A., Dazlich, D. A., Los, S. O., ... Jensen, T. G. (1996, March). Comparison of Radiative and Physiological Effects of Doubled Atmospheric CO2 on Climate. *Science*, *271*(5254), 1402–1406. Retrieved 2020-02-03, from http://www.sciencemag.org/cgi/doi/10.1126/science.271.5254.1402 doi: 10.1126/science.271.5254.1402
Seneviratne, S. I., Wilhelm, M., Stanelle, T., van den Hurk, B., Hagemann, S., Berg, A., ... Smith, B. (2013). Impact of soil moisture-climate feedbacks on CMIP5 projections: First results from the GLACE-CMIP5 experiment. *Geophysical Research Letters*, *40*(19), 5212–5217. Retrieved 2023-06-05, from https://onlinelibrary.wiley.com/doi/abs/10.1002/grl.50956 (_eprint: https://onlinelibrary.wiley.com/doi/pdf/10.1002/grl.50956) doi: 10.1002/grl.50956
Sexton, D. M. H., McSweeney, C. F., Rostron, J. W., Yamazaki, K., Booth, B. B. B., Murphy, J. M., ... Karmalkar, A. V. (2021, June). A perturbed parameter ensemble of HadGEM3-GC3.05 coupled model projections: part 1: selecting the parameter combinations. *Climate Dynamics*, *56*(11), 3395–3436. Retrieved 2023-06-10, from https://doi.org/10.1007/s00382-021-05709-9 doi: 10.1007/s00382-021-05709-9
Shukla, J., & Mintz, Y. (1982). Influence of Land-Surface Evapotranspiration on the Earth's Climate. *Science*, *215*(4539), 1498–1501. Retrieved 2022-09-29, from https://www.jstor.org/stable/1688150 (Publisher: American Association for the Advancement of Science)
Smith, N. G., Lombardozzi, D., Tawfik, A., Bonan, G., & Dukes, J. S. (2017). Biophysical consequences of photosynthetic temperature acclimation for climate. *Journal of Advances in Modeling Earth Systems*, *9*(1), 536–547. Retrieved 2021-02-20, from https://agupubs.onlinelibrary.wiley.com/doi/abs/10.1002/2016MS000732 doi: https://doi.org/10.1002/2016MS000732
Sud, Y. C., Shukla, J., & Mintz, Y. (1988, September). Influence of Land Surface Roughness on Atmospheric Circulation and Precipitation: A Sensitivity Study with a General Circulation Model. *Journal of Applied Me-*

teorology and Climatology, *27*(9), 1036–1054. Retrieved 2023-02-15, from https://journals.ametsoc.org/view/journals/apme/27/9/1520-0450_1988_027_1036_iolsro_2_0_co_2.xml (Publisher: American Meteorological Society Section: Journal of Applied Meteorology and Climatology) doi: 10.1175/1520-0450(1988)027⟨1036:IOLSRO⟩2.0.CO;2

Swann, A. L. S., Fung, I. Y., & Chiang, J. C. H. (2012, January). Mid-latitude afforestation shifts general circulation and tropical precipitation. *Proceedings of the National Academy of Sciences*, *109*(3), 712–716. Retrieved 2019-12-30, from https://www.pnas.org/content/109/3/712 doi: 10.1073/pnas.1116706108

Tett, S. F. B., Gregory, J. M., Freychet, N., Cartis, C., Mineter, M. J., & Roberts, L. (2022, April). Does Model Calibration Reduce Uncertainty in Climate Projections? *Journal of Climate*, *35*(8), 2585–2602. Retrieved 2023-02-23, from https://journals.ametsoc.org/view/journals/clim/35/8/JCLI-D-21-0434.1.xml (Publisher: American Meteorological Society Section: Journal of Climate) doi: 10.1175/JCLI-D-21-0434.1

Voosen, P. (2020, October). Europe builds 'digital twin' of Earth to hone climate forecasts. *Science*, *370*(6512), 16–17. Retrieved 2023-05-30, from https://www.science.org/doi/full/10.1126/science.370.6512.16 (Publisher: American Association for the Advancement of Science) doi: 10.1126/science.370.6512.16

Williams, I. N., Lu, Y., Kueppers, L. M., Riley, W. J., Biraud, S. C., Bagley, J. E., & Torn, M. S. (2016). Land-atmosphere coupling and climate prediction over the U.S. Southern Great Plains. *Journal of Geophysical Research: Atmospheres*, *121*(20), 12,125–12,144. Retrieved 2022-11-02, from https://onlinelibrary.wiley.com/doi/abs/10.1002/2016JD025223 (_eprint: https://onlinelibrary.wiley.com/doi/pdf/10.1002/2016JD025223) doi: 10.1002/2016JD025223

Yamazaki, K., Sexton, D. M. H., Rostron, J. W., McSweeney, C. F., Murphy, J. M., & Harris, G. R. (2021, June). A perturbed parameter ensemble of HadGEM3-GC3.05 coupled model projections: part 2: global performance and future changes. *Climate Dynamics*, *56*(11), 3437–3471. Retrieved 2023-01-30, from https://doi.org/10.1007/s00382-020-05608-5 doi: 10.1007/s00382-020-05608-5

Zaehle, S., Sitch, S., Smith, B., & Hatterman, F. (2005). Effects of parameter uncertainties on the modeling of terrestrial biosphere dynamics. *Global Biogeochemical Cycles*, *19*(3). Retrieved 2022-11-02, from https://onlinelibrary.wiley.com/doi/abs/10.1029/2004GB002395 (_eprint: https://onlinelibrary.wiley.com/doi/pdf/10.1029/2004GB002395) doi: 10.1029/2004GB002395

Zhang, C., Xie, S., Klein, S. A., Ma, H.-y., Tang, S., Van Weverberg, K., … Petch, J. (2018). CAUSES: Diagnosis of the Summertime Warm Bias in CMIP5 Climate Models at the ARM Southern Great Plains Site. *Journal of Geophysical Research: Atmospheres*, *123*(6), 2968–2992. Retrieved 2023-12-28, from https://onlinelibrary.wiley.com/doi/abs/10.1002/2017JD027200 (_eprint: https://onlinelibrary.wiley.com/doi/pdf/10.1002/2017JD027200) doi: 10.1002/2017JD027200

Zheng, Y., Kumar, A., & Niyogi, D. (2015, May). Impacts of land–atmosphere coupling on regional rainfall and convection. *Climate Dynamics*, *44*(9), 2383–2409. Retrieved 2024-01-16, from https://doi.org/10.1007/s00382-014-2442-8 doi: 10.1007/s00382-014-2442-8

Supplementary Material for "Land Processes Can Substantially Impact the Mean Climate State"

Claire M. Zarakas[1], Daniel Kennedy[3], Katherine Dagon[3], David M. Lawrence[3], Amy Liu[1], Gordon Bonan[3], Charles Koven[4], Danica Lombardozzi[3], and Abigail L. S. Swann[1,2]

[1]University of Washington, Department of Atmospheric Sciences
[2]University of Washington, Department of Biology
[3]National Center for Atmospheric Research
[4]Lawrence Berkeley National Laboratory

Contents of this file

1. Text S1 to S4
2. Figures S1 to S15
3. Tables S1 to S4

Text S1 Model configuration and experimental design

CESM PPE simulations were run using the `branch_tags/PPE.n11_ctsm5.1.dev030` tag for the Community Land Model version 5 (CLM5; Lawrence et al., 2019) and the `cesm2.2.0` tag for all other model components. The land was initialized with the spun-up land state from the default model parameterization which includes the carbon content of soil and vegetation pools. The coupled simulations use the Community Atmosphere Model 6 (CAM6; Bogenschutz et al., 2018), and a slab ocean (Danabasoglu & Gent, 2009) which is based on q-fluxes from preindustrial simulations of the full dynamic ocean model. We did not apply flux corrections, and note that the top of atmosphere energy imbalance is relatively small and changes minimally across the PPE (average=-0.157 W/m^2, σ=0.010 W/m^2; Figure S14).

Each parameter perturbation simulation, which we refer to as an ensemble member, was run for 140 years under constant preindustrial greenhouse gas concentrations and land use conditions. The first 40 years were discarded as spin up, which is long enough for fast atmospheric processes, leaf area, soil moisture and temperature, and the surface ocean to largely equilibrate (Figure S15).

Text S2 Parameter selection procedure

We used two parameter selection criteria: (1) that parameters would likely have a large impact on the atmosphere, based on results from the CLM5 PPE, and (2) that parameters sampled different functional areas of the model. For our first criterion, we ranked all parameters based on multiple metrics of land-to-atmosphere fluxes (Table S1, Table S3), globally and for individual biomes, focusing on the quantities that the land model passes to the atmosphere model in CESM2 (Table S2). We quantified parameters impact on individual biomes by classifying the land surface into the nine Whittaker biomes (Whittaker, 1975) and ice sheets based on each grid cell's mean precipitation and temperature. Out of 205 total parameters, we identified 40 parameters that appeared in the top five for more than five rankings. For our second criterion, we then grouped those top 40 parameters into functional categories, and we selected 18 parameters such that we did not sample more than four parameters from any given functional category.

Text S3 Calculating the pattern of warming due to a doubling of CO_2

We calculated the pattern of warming due to a doubling of CO_2 from two concentration-driven CESM2 simulations: one forced with preindustrial CO_2 concentrations of 284.7 ppm (1xCO_2) and one forced with a doubling of preindustrial CO_2, 569.4 ppm (2xCO_2). We ran simulations with an active land and atmosphere, and a slab ocean. We ran simulations for 120 years, and discarded the first 60 years as spin up. These CESM simulations were run using the `cesm_2_3_beta03` tag and `branch_tags/PPE.n08_ctsm5.1.dev030` tag for CTSM. Doubling CO_2 drove a 5.2°C global mean temperature increase (6.5°C global mean land temperature increase), consistent with CESM2's documented high equilibrium climate sensitivity (Gettelman et al. 2019).

Text S4 Disentangling drivers of land temperature and precipitation changes

We used multiple linear regression to disentangle the extent to which land precipitation (P) and temperature (T_s) changes across our coupled PPE are driven by three land surface properties: albedo (α), evaporative fraction (EF), and a measure of aerodynamic coupling (r_a). First, we diagnosed α, EF, and r_a for each ensemble member of land-only PPE at each grid cell using monthly model output. We calculated r_a by inverting the equation for sensible heat flux. We then use these derived changes in land-only α, EF, r_a as predictors in a multiple linear regression to predict coupled T_s and P change at each point for each month. We used predictors from the land-only rather than the coupled PPE in order to remove the feedback between climate and land surface properties. In the coupled PPE, changes in land surface properties are due to both land parameter uncertainty and land responses to climate changes (e.g., precipitation changes can influence evaporative fraction), but changes in land surface properties in the land-only PPE isolate the influence of land parameter uncertainty on land surface fluxes. Because this grid cell level analysis does not account for remote or global-scale impacts of parameter perturbations, we also report results from regressions conducted using global averages. We do not perform regressions on global average land precipitation changes because the sign of precipitation changes are more regionally variable.

We calculated the emergent changes in r_s and r_a by inverting the equations for sensible heat flux and latent heat flux (L). S=$(\rho C_p(T_s - T_a))/r_a$ and L=$(\rho\lambda(q^*(T_s) - q_a))/(r_a + r_s)$, where ρ is the air density at the lowest atmospheric level, T_a is the air temperature at the lowest atmospheric level, q_a is the specific humidity at the lowest atmospheric level, T_s is land surface skin temperature, and $q^*(T_s)$is the saturated specific humidity at T_s. C_p and λ are constants, the specific heat capacity of dry air and the latent heat of vaporization, respectively. We verified our derived changes in α, r_s, and r_a by demonstrating that they yielded accurate reconstructions of temperature changes in the offline land-only PPE using the two-resistance method (TRM; Rigden and Li 2017). However, the TRM is ill-suited for attributing quantifying how much the changes in α, r_s, and r_a drive coupled temperature changes to changes in α, r_s, and r_a because it combines all temperature changes from atmospheric feedbacks into one term (due to change in the near-surface air temperature T_a), and cannot distinguish the extent to which T_a changes are driven by changes in α, r_s, and r_a.

References

Bogenschutz, P. A., Gettelman, A., Hannay, C., Larson, V. E., Neale, R. B., Craig, C., & Chen, C.-C. (2018, January). The path to CAM6: coupled simulations with CAM5.4 and CAM5.5. *Geoscientific Model Development*, *11*(1), 235–255. Retrieved 2023-06-10, from `https://gmd.copernicus.org/articles/11/235/2018/` (Publisher: Copernicus GmbH) doi: 10.5194/gmd-11-235-2018

Danabasoglu, G., & Gent, P. R. (2009, May). Equilibrium Climate Sensitivity: Is It Accurate to Use a Slab Ocean Model? *Journal of Climate*, *22*(9), 2494–2499. Retrieved 2023-11-15, from `https://journals.ametsoc.org/view/journals/clim/22/9/2008jcli2596.1.xml` (Publisher: American Meteorological Society Section: Journal of Climate) doi: 10.1175/2008JCLI2596.1

Lawrence, D. M., Fisher, R. A., Koven, C. D., Oleson, K. W., Swenson, S. C., Bonan, G., ... Zeng, X. (2019). The Community Land Model Version 5: Description of New Features, Benchmarking, and Impact of Forcing Uncertainty. *Journal of Advances in Modeling Earth Systems*, *11*, 4245–4287. Retrieved 2019-12-28, from `https://agupubs.onlinelibrary.wiley.com/doi/abs/10.1029/2018MS001583` doi: 10.1029/2018MS001583

Whittaker, R. H. (1975). *Communities and Ecosystems* (2nd ed.). New York: MacMillan.

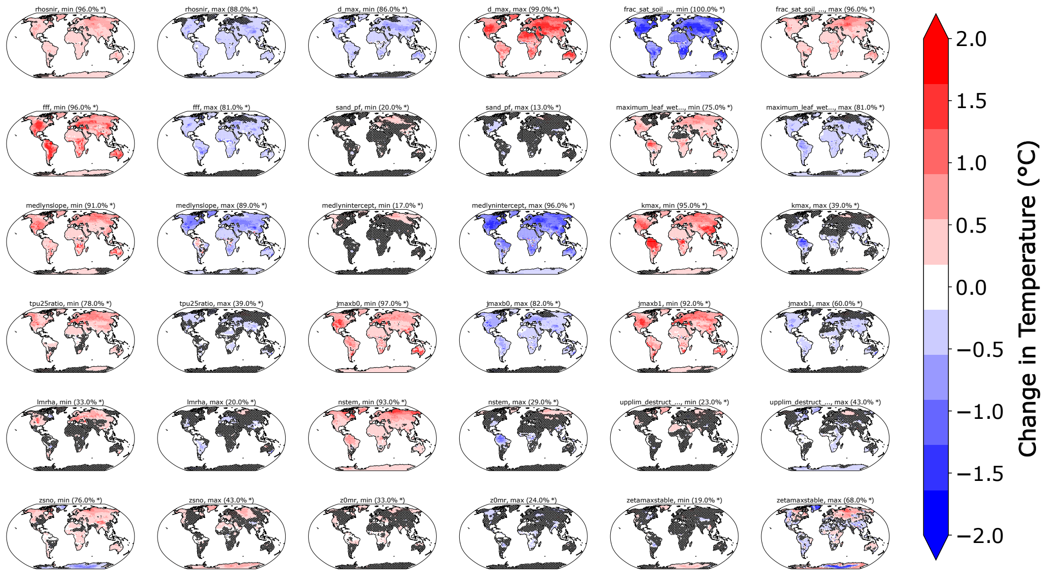

Figure S1: Maps of annual mean land temperature changes for each ensemble member, compared to the reference case with default parameterizations. Hatching indicates regions where the temperature change was insignificant at the 0.05 significance level. The percentage of land with statistically significant temperature changes is shown in parentheses, and * indicates field significance. For each grid cell, we performed a two-tailed Student's t-test to test whether the ensemble member mean (standard deviation calculated from the distribution from interannual variability in the ensemble member mean) was different from the default mean (standard deviation calculated from the distribution from interannual variability in the default mean). We test for field significance using Walker's test.

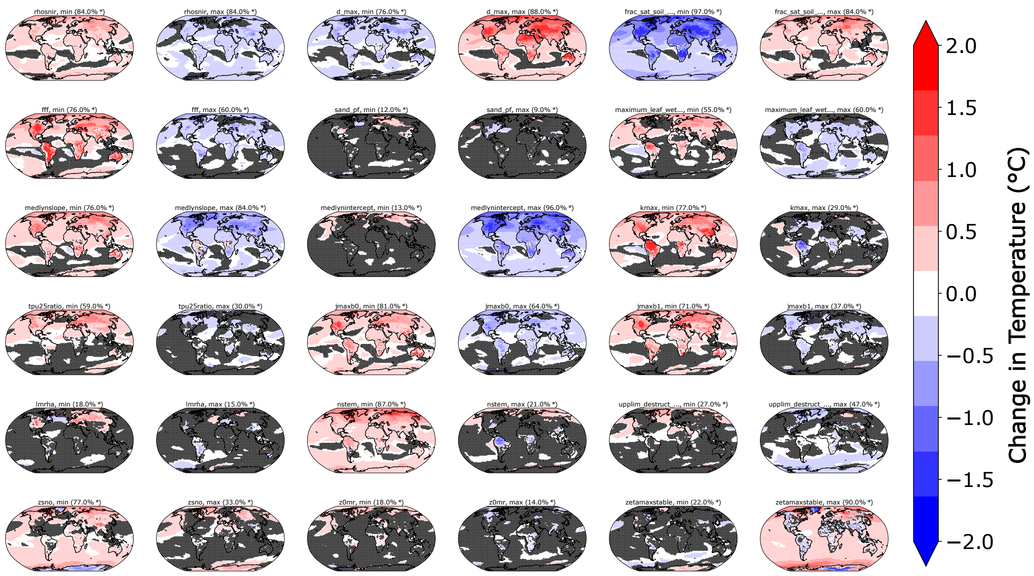

Figure S2: Maps of annual mean temperature changes for each ensemble member, including both land and ocean. Hatching and significance testing is as in Figure S1, but the title indicates the total percentage of the Earth surface (including land and ocean) with statistically significant temperature changes.

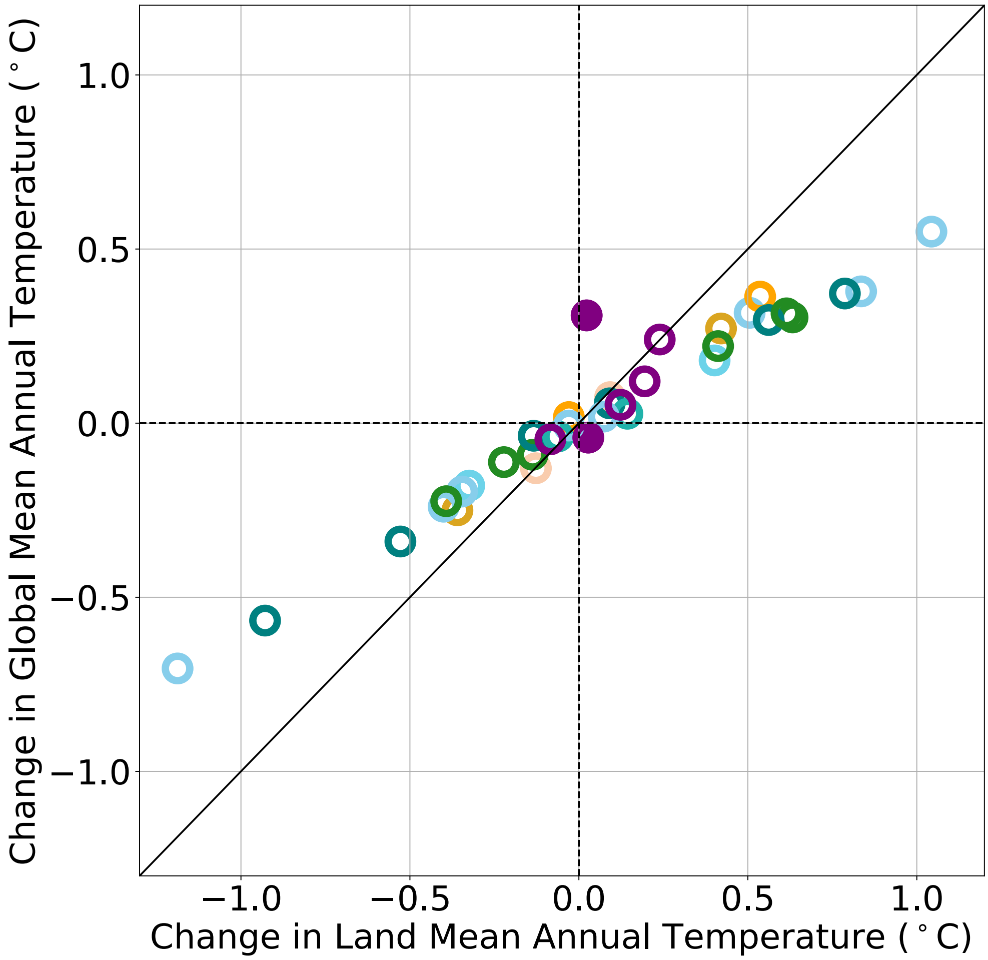

Figure S3: Correlation between the change in annual mean land temperature and annual mean global temperature (including both land and ocean). Colors indicate parameter category as in Figures 1 and 3. Because the parameter `zetamaxstable` is an outlier in our PPE, it is denoted as the filled purple point.

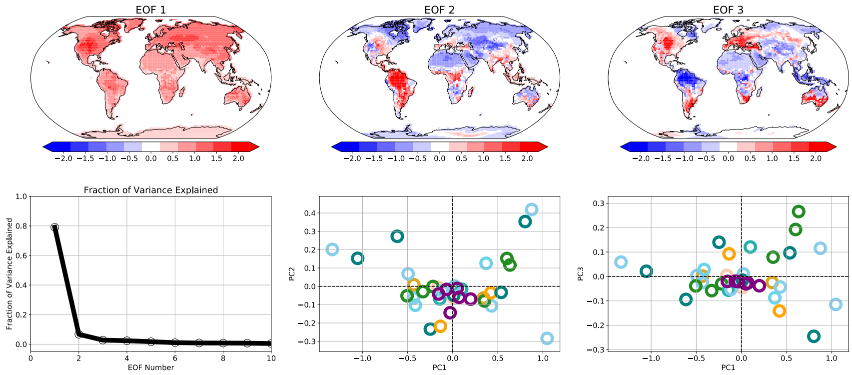

Figure S4: EOF analysis of changes in land surface temperature across the PPE.

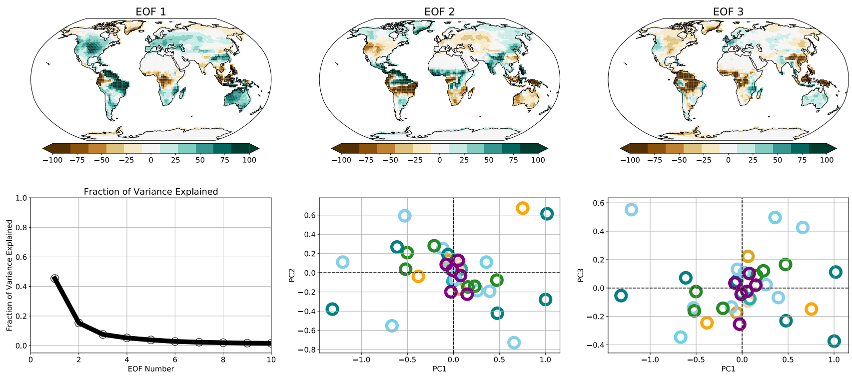

Figure S5: EOF analysis of changes in land precipitation across the PPE.

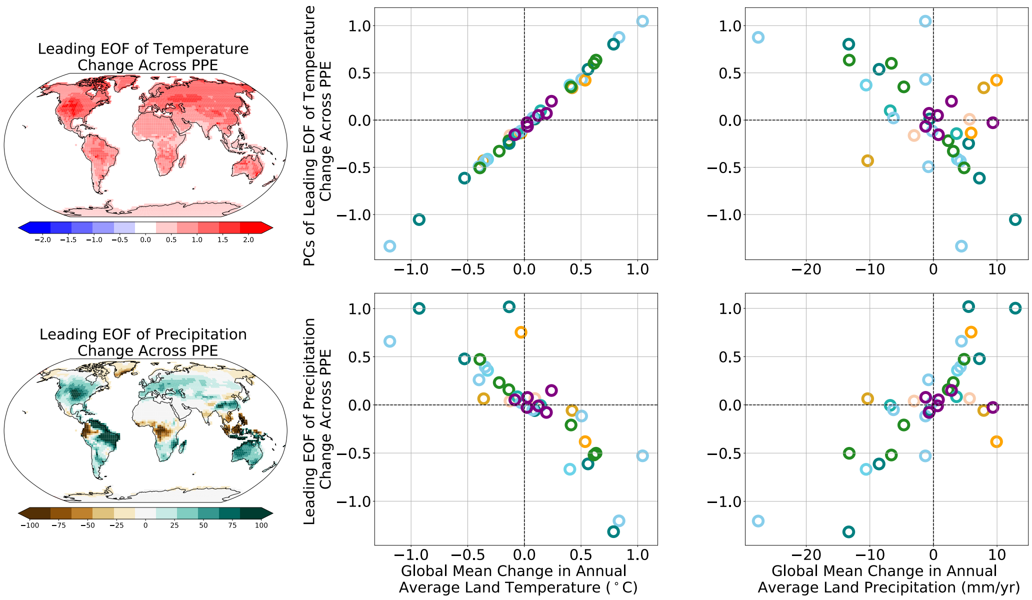

Figure S6: Correlation between leading EOFs of annual average land and temperature changes and global mean annual average land temperature and precipitation changes across the PPE. Ensemble members are colored by parameter category, as in Figure 1.

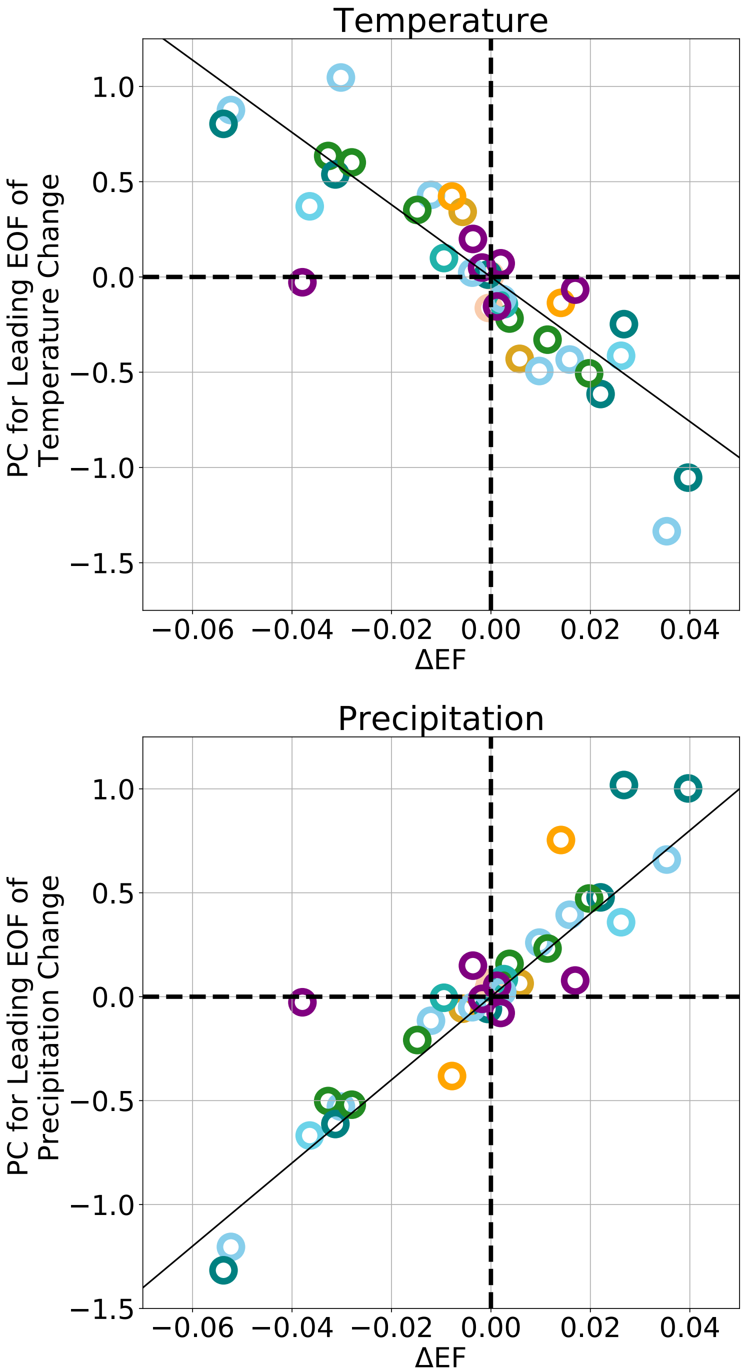

Figure S7: Correlation between change in global mean evaporative fraction (EF) and first principal components of temperature (top) and precipitation (bottom) change across the PPE. Colors indicate parameter category as in Figure 1.

Figure S8: Maps of annual mean land precipitation changes for each ensemble member, compared to the reference case with default parameterizations. Hatching indicates regions where the precipitation change was insignificant at the 0.05 significance level. The percentage of land with statistically significant temperature changes are shown in parentheses, and * indicates field significance.For each grid cell, we performed a two-tailed Student's t-test to test whether the ensemble member mean (standard deviation calculated from the distribution from interannual variability in the ensemble member mean) was different from the default mean (standard deviation calculated from the distribution from interannual variability in the default mean). We test for field significance using Walker's test.

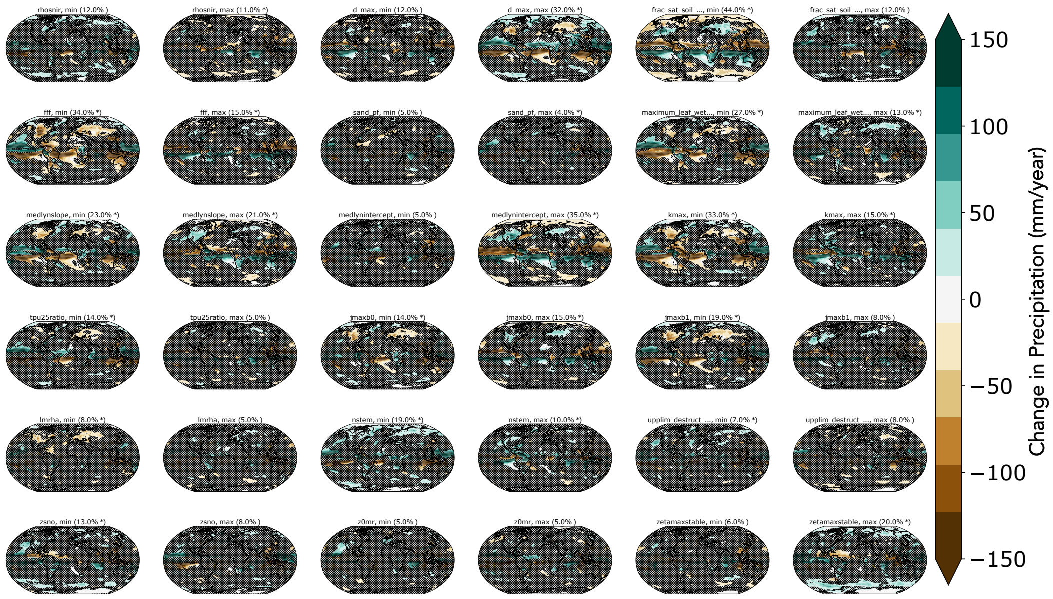

Figure S9: Maps of annual mean precipitation changes for each ensemble member, including both land and ocean. Hatching and significance testing is as in Figure S7, but the title indicates the total percentage of the Earth surface (including land and ocean) with statistically significant temperature changes.

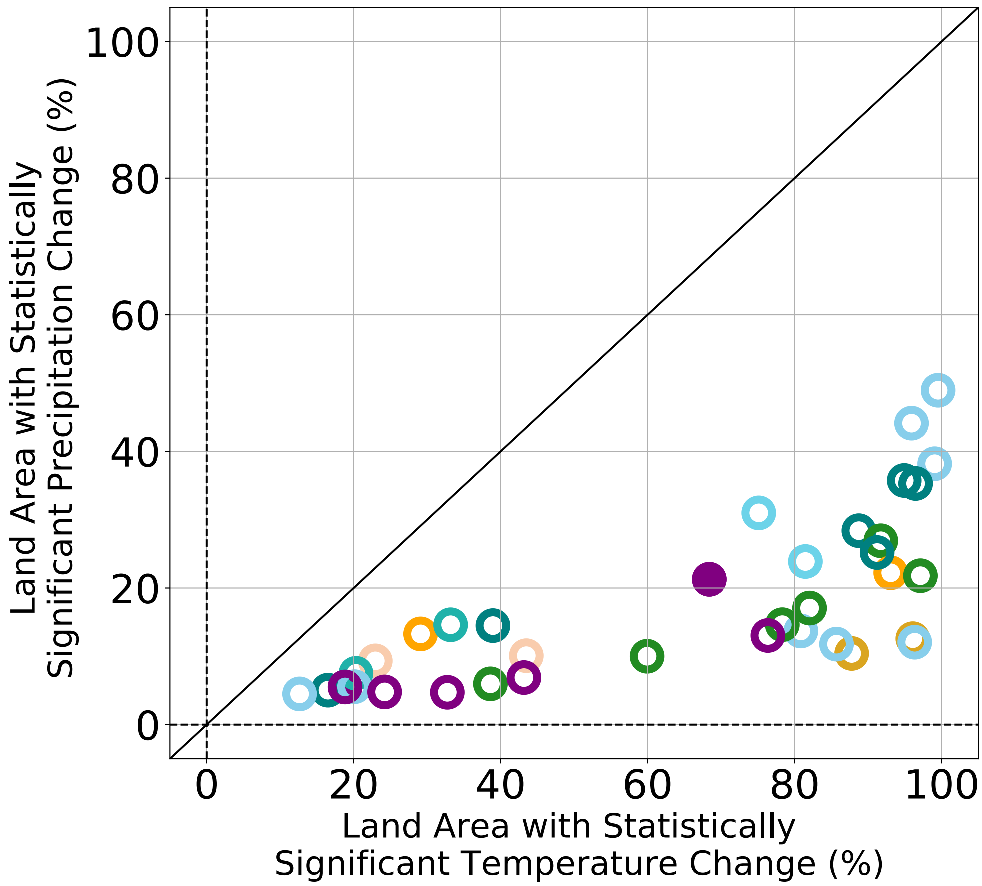

Figure S10: Percentage of land area with statistically significant temperature vs. precipitation changes for each ensemble member in the PPE. Ensemble members are colored by parameter category, as in Figure 1. Zetamaxstable is indicated with a filled circle because it is a frequent outlier.

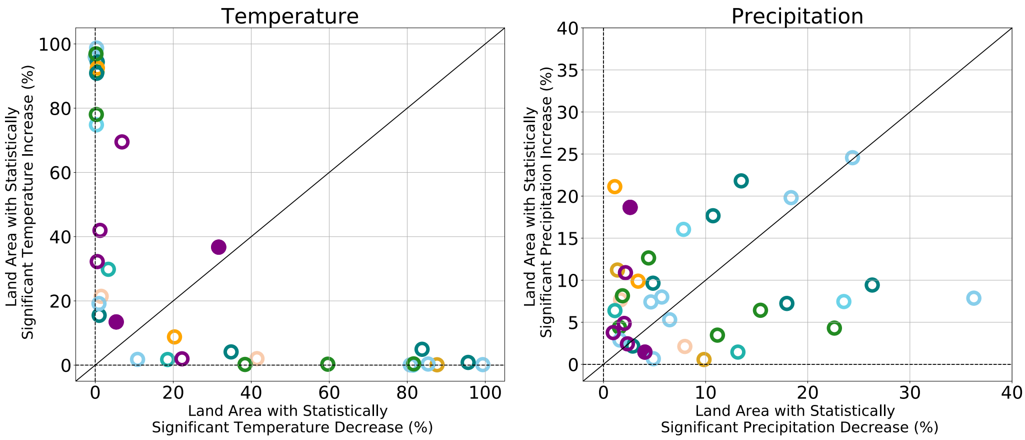

Figure S11: Sign of change of statistically significant mean climate changes across the PPE. Percent of land area experiencing statistically significant decreases vs. increases in temperature (left) and precipitation (right) for each PPE ensemble member. Ensemble members are colored by parameter category, as in Figure 1. We note that one parameter (`zetamaxstable`) drove statistically significant temperature changes of opposite sign across 63% of land area, which canceled each other out in the global mean resulting in a minimal global mean land temperature change (Figure S1) - this parameter is indicated with a filled circle because it is a frequent outlier.

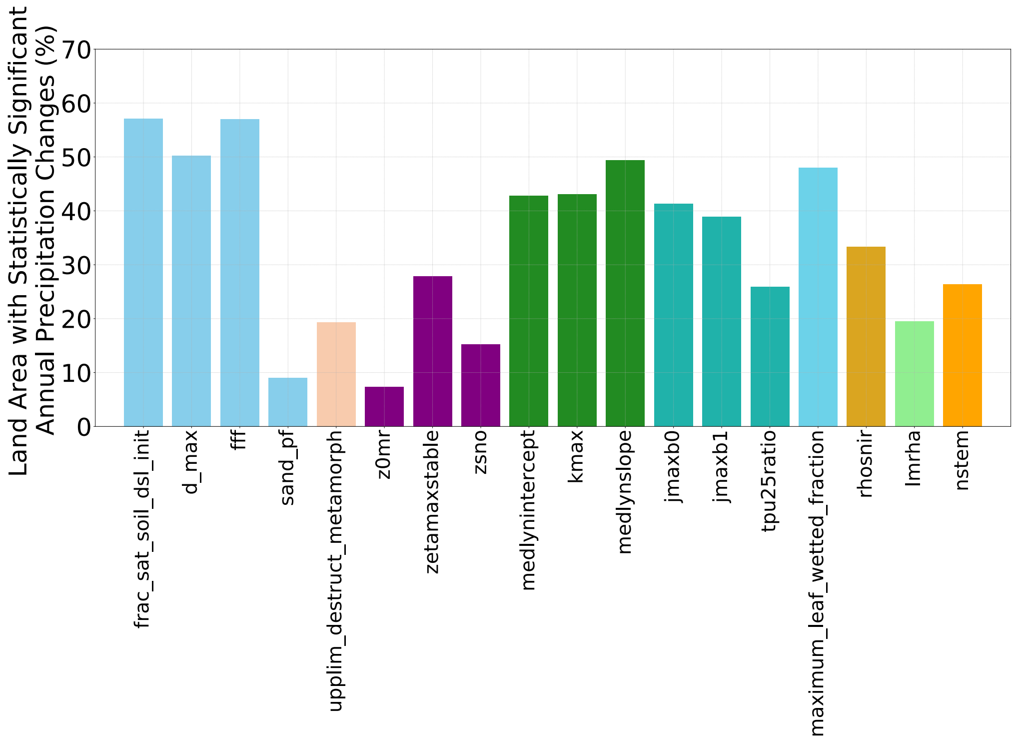

Figure S12: Percentage of global land area that experiences statistically significant changes in annual mean precipitation due to perturbations in each parameter. For each land grid cell, we performed a two-tailed Student's t-test to test whether the parameter maximum simulation was different from the parameter minimum simulation.

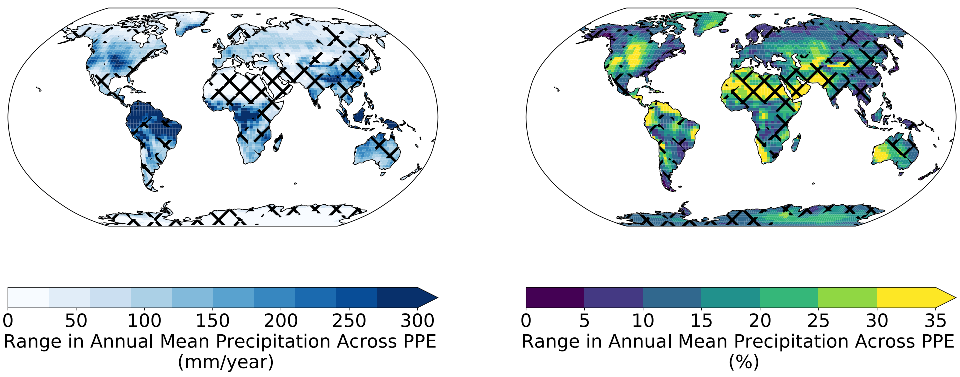

Figure S13: Range in annual mean precipitation changes across the PPE, on an absolute basis (left) and as a percentage of the default precipitation (right). Hatching indicates regions where annual mean precipitation changes were statistically insignificant for five or more ensemble members.

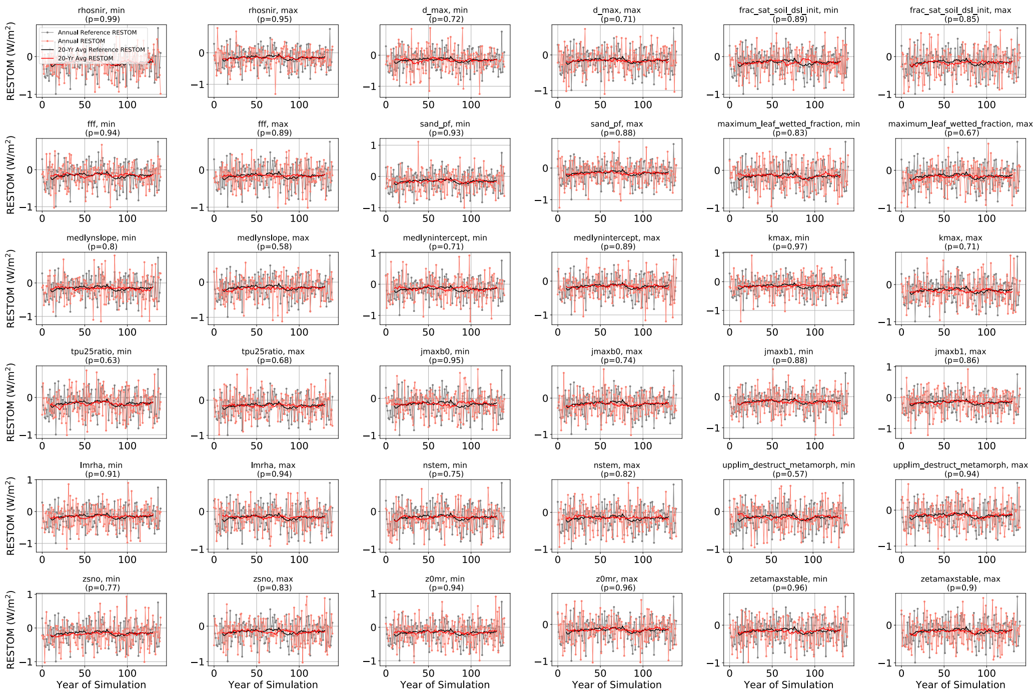

Figure S14: Time series of the net radiative flux at the top of the model (RESTOM), as calculated from the net solar flux at top of model (FSNT) minus the net longwave flux at top of model (FLNT). The average RESTOM for the last 100 years of the reference case is -0.15 W/m^2. RESTOM varied minimally across the ensemble (σ=0.010 W/m^2), and was not statistically significantly different from the reference case for any ensemble member. Significance was tested using two-tailed Student's t-test on the time series of annual mean RESTOM.

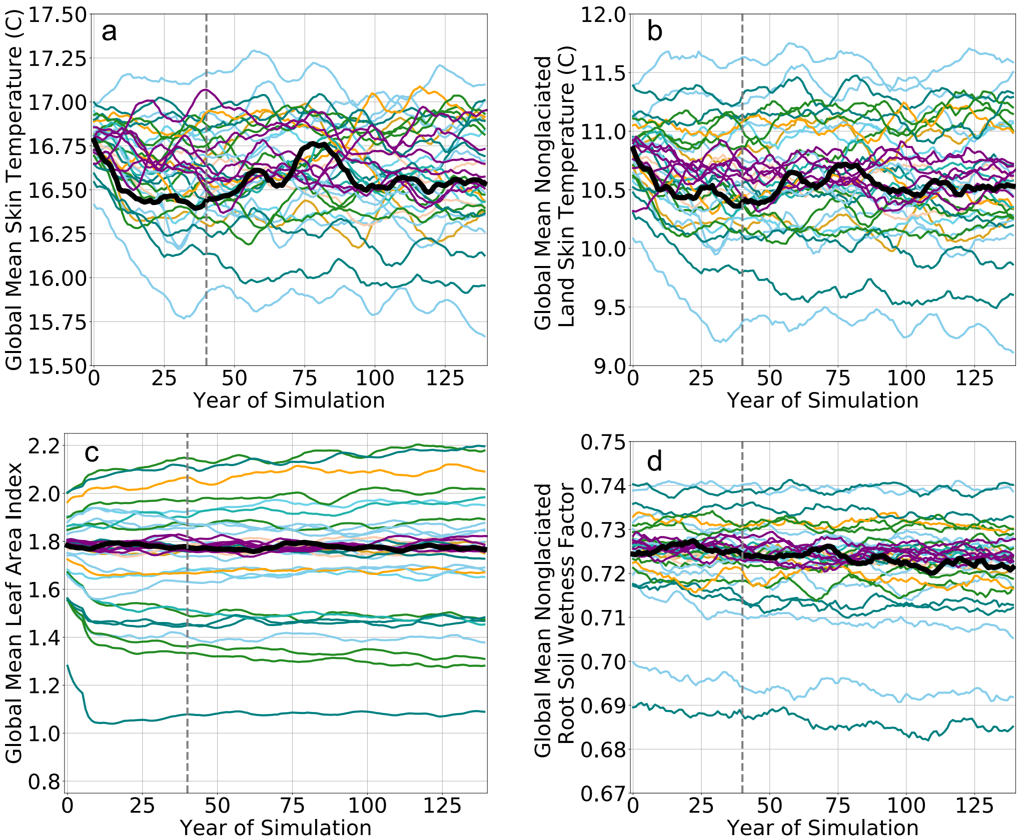

Figure S15: Time series of annual mean (a) global temperature, (b) global land temperature, (c) global leaf area index, and (d) global root zone soil wetness factor (where 1 indicates no water stress) for each ensemble member of the PPE. The black line indicates the reference simulations, and ensemble members are colored by parameter category as in Figure 1. The first 40 years of each simulation (denoted by dashed vertical line) were discarded as spin up. Data in panels (c) and (d) are averaged over non-glaciated land only.

Quantity
Latent heat flux
Sensible heat flux
Water vapor flux
Zonal momentum flux
Meriodional momentum flux
Emitted longwave radiation
Direct beam visible albedo
Direct beam near-infrared albedo
Diffuse visible albedo
Diffuse near-infrared albedo
Absorbed solar radiation
Radiative temperature
Temperature at 2 meter height
Specific humidity at 2 meter height
Wind speed at 10 meter height
Snow water equivalent
Aerodynamic resistance
Friction velocity
Dust flux
Net ecosystem exchange*

Table S1: Quantities that the land model passes to the atmosphere in CESM2. Note that net ecosystem exchange does not impact the atmosphere in our experimental design because our experimental design held atmospheric CO_2 concentrations fixed.

Metric	CLM5 Variable	Metric Category	Measure	Globally	By Whittaker Biome
Annual Mean					
Mean albedo	Calculated quantity	Albedo and shortwave radiation	Mean	Yes	Yes
Mean absorbed shortwave radiation	FSA		Mean	Yes	Yes
Mean emitted longwave radiation	FIRE	Temperature and longwave radiation	Mean	Yes	Yes
Mean near-surface air temperature	TSA		Mean	Yes	Yes
Mean land skin temperature	TSKIN		Mean	Yes	Yes
Mean latent heat flux	EFLX_LH_TOT	Water and turbulent fluxes	Mean	Yes	Yes
Mean sensible heat flux	FSH		Mean	Yes	Yes
Mean near-surface specific humidity	Q2M		Mean	Yes	Yes
Mean zonal momentum flux	TAUX	Wind and roughness	Mean	Yes	Yes
Mean 10 meter wind speed	U10		Mean	Yes	Yes
LAC Area (DJF)	Calculated quantity*	Land-atmosphere coupling (LAC)	Mean	Yes	No
LAC Area (JJA)	Calculated quantity*		Mean	Yes	No
LAC Area (MAM)	Calculated quantity*		Mean	Yes	No
LAC Area (SON)	Calculated quantity*		Mean	Yes	No
Interannual Variability					
Mean albedo	Calculated quantity*	Albedo and shortwave radiation	IAV	Yes	Yes
Mean absorbed shortwave radiation	FSA		IAV	Yes	Yes
Mean emitted longwave radiation	FIRE	Temperature and longwave radiation	IAV	Yes	Yes
Mean near-surface air temperature	TSA		IAV	Yes	Yes
Mean land skin temperature	TSKIN		IAV	Yes	Yes
Mean latent heat flux	EFLX_LH_TOT	Water and turbulent fluxes	IAV	Yes	Yes
Mean sensible heat flux	FSH		IAV	Yes	Yes
Mean near-surface specific humidity	Q2M		IAV	Yes	Yes
Mean zonal momentum flux	TAUX	Wind and roughness	IAV	Yes	Yes
Mean 10 meter wind speed	U10		IAV	Yes	Yes

Table S2: Metrics for evaluating parameter impact on land-to-atmosphere fluxes.

Parameters	Global Ranking	Biome Ranking									
		Tropical rain forest	Tropical seasonal forest/savanna	Temperate rain forest	Temperate seasonal forest	Woodland/ shrubland	Temperate grassland/ desert	Subtropical desert	Boreal forest	Tundra	Ice sheet
kmax	1	1	1	-	3	3	4	4	4	4	-
medlynslope	3	-	4	-	1	5		5	1	1	-
fff	2	-	2	-		1	1	1		2	-
medlynintercept	5	5	3	5	2	-	-	-	2		-
liq_canopy_storage_scalar	4	2	5	-	4	-	-	-	3		-
jmaxb0	-	-	-	4	-	-	-	-	5	3	-
jmaxb1	-	-	-	3	5	2	-	-	-	-	-
tpu25ratio	-	-	-	2	-	4	-	-	-	-	-
sand_pf	-	-	-		-	-	5	3	-	-	-
maximum_leaf_wetted_fraction	-	3	-	1	-	-	-	-	-	-	-
krmax	-	-	-	-	-	-	2	2	-	-	-
snw_rds_refrz	-	-	-	-	-	-	-	-	-	-	3
upplim_destruct_metamorph	-	-	-	-	-	-	-	-	-	-	4
slopebeta	-	-	-	-	-	-	-	-	-	5	-
zetamaxstable	-	-	-	-	-	-	-	-	-	-	1
zsno	-	-	-	-	-	-	-	-	-	-	2
d_max	-	-	-	-	-	-	3	-	-	-	-
psi50	-	4	-	-	-	-	-	-	-	-	-

Table S3: Example of parameter rankings in terms of their impact on mean latent heat flux, globally and for Whittaker biomes. Rankings are only shown if the parameter was ranked in the top 5. Bolded parameters were included in our PPE.

Parameters	Global Ranking	Biome Ranking									
		Tropical rain forest	Tropical seasonal forest/savanna	Temperate rain forest	Temperate seasonal forest	Woodland/ shrubland	Temperate grassland/ desert	Subtropical desert	Boreal forest	Tundra	Ice sheet
fff	1	-	1	-	-	1	-	4	-	-	-
zetamaxstable	2	-	-	-	-		4	-	1	1	1
jmaxb0	3	-	-	5	3	-	-	5	3	4	-
kmax	4	1	2	-	2	-	-	-	5	-	-
leafcn	5	-	-	-	5	-	-	-	-	-	-
jmaxb1	-	-	-	2	1	2	-	-	2	-	-
tpu25ratio	-	-	-	1	4	4	-	-	4	-	-
zsno	-	-	-	-	-	-	1	-	-	2	2
clay_pf	-	-	-	-	-	-	3	2	-	-	-
leaf_long	-	4	5	-	-	-			-	-	-
maximum_leaf_wetted_fraction	-	2	-	3	-	-			-	-	-
sand_pf	-	-	-	-	-	-	2	3	-	-	-
d_max	-	-	-	-	-	-	5	-	-	-	-
frac_sat_soil_dsl_init	-	-	3	-	-	-	-	-	-	-	-
FUN_fracfixers	-	-	-	-	-	3	-	-	-	-	-
krmax	-	-	4	-	-	-	-	-	-	-	-
liq_canopy_storage_scalar	-	3	-	-	-	-	-	-	-	-	-
lmrha	-	-	-	-	-	5	-	-	-	-	-
medlynintercept	-	-	-	-	-	-	-	-	-	5	-
medlynslope	-	-	-	-	-	-	-	-	-	3	-
psi50	-	5	-	-	-	-	-	-	-	-	-
snw_rds_refrz	-	-	-	-	-	-	-	-	-	-	4
tpuha	-	-	-	4	-	-	-	-	-	-	-
upplim_destruct_metamorph	-	-	-	-	-	-	-	-	-	-	5
xdrdt	-	-	-	-	-	-	-	-	-	-	3
zlnd	-	-	-	-	-	-	-	1	-	-	-

Table S4: Rankings of parameters with the largest land surface temperature change in the land-only CLM5-PPE, globally and for Whittaker biomes. Rankings are only shown if the parameter was ranked in the top 5. Bolded parameters were included in our PPE, and parameters relating to soil hydrology, stomatal conductance and plant water use, and canopy evaporation are highlighted.

Parameter	Parameter description	Land Component	Parameter Category	Minimum Value	Default Value	Maximum Value	Unit	Range source	Reference
`d_max`	Parameter specifying the length scale of max dry surface layer thickness	Soil	Soil hydrology	10	15	60	mm	Literature review	Swenson and Lawrence (2014), van de Griend and Owe (1994), Goss and Madliger (2007), Smits et al. (2012)
`frac_sat_soil_dsl_init`	Fraction of saturated soil for moisture value at which dry surface layer initiates			0.5	0.8	1	unitless	Literature review	Swenson and Lawrence (2014)
`fff`	Decay factor for fractional saturated area			0.02	0.5	5	m^{-1}	Literature review	Niu et al. (2005), Hou et al. (2012), Fan and Miguez-Macho (2011), Fan et al. (2013)
`sand_pf`	Perturbation factor (via addition) for percent sand			-20	0	20	percent	Percentage perturbation	
`z0mr`	Ratio of momentum roughness length to canopy top height	Boundary layer	Boundary layer / Roughness length	0.033 to 0.072^a	0.055 to 0.120^a	0.077 to 0.168^a	unitless	Literature review	Zeng and Wang (2007), Raupach (1994), Shaw and Pereira (1982)
`zsno`	Momentum roughness length for snow			0.00001	0.0024	0.07	m	Literature review	Chamberlain (1983), Manes et al. (2008), Gromke et al. (2011)
`zetamaxstable`	Max value zeta ("height" used in Monin-Obukhov theory) can go to under stable conditions.*			0.1	0.5	10	unitless	Expert judgment	
`upplim_destruct_metamorph`	Upper limit for snow densification through destructive metamorphism		Snow	100	175	250	kg/m^3	Literature review	van Kampenhout et al. (2017)
`jmaxb0`	Tthe baseline proportion of nitrogen allocated for electron transport	Vegetation	Photosynthesis	0.01	0.0311	0.05	J	Expert judgment	
`jmaxb1`	Determines the response of electron transport rate to light availability			0.05	0.17	0.25	unitless	Expert judgment	
`tpu25ratio`	Triose phosphate utilization at 25C (ratio of tpu25/vcmax25)			0.0835	0.167	0.501	unitless	Percentage perturbation	Lombardozzi et al., GRL (2018)
`lmrha`	Activation energy for leaf maintenance respiration (used in temperature acclimation of leaf maintenance respiration)		Temperature acclimation	-50%	46390	+50%	J/mol	Percentage perturbation	Bernacchi et al. (2001)
`medlynslope`	Medlyn slope of conductance-photosynthesis relationship		Stomatal conductance and plant water use	0.65 to 3.89^a	1.62 to 5.79^a	3.93 to 9.11^a	μmol H_2O/ μmol CO_2	Literature review	Lin et al. (2015)
`medlynintercept`	Medlyn intercept of conductance-photosynthesis relationship			1	100	200000	μmol H_2O/(m^2/s)	Literature review	Duursma et al. (2018)
`kmax`	Plant segment maximum conductance			2.3e-10 to $1.5e\text{-}8^a$	1.3e-9 to $4.0e\text{-}8^a$	1.9e-9 to $2.3e\text{-}7^a$	mm H_2O (transpired)/ mm H_2O (water potential gradient)/sec	Literature review	Bonan et al. (2014), Chuang et al. (2006), Sperry et al. (1998), Sperry and Love (2015), Williams et al (1996), Kennedy et al. (2019)
`rhosnir`	Near-infrared stem reflectance		Plant optical properties	0.29 to 0.42^a	0.36 to 0.53^a	0.43 to 0.64^a	unitless	Percentage perturbation	Majasalmi and Bright (2019)
`maximum_leaf_wetted_fraction`	Maximum fraction of leaf that may be wet prior to drip occuringoccurring		Canopy evaporation	0.01	0.05	0.5	unitless	Expert judgment	
`nstem`	Stem number; number of individuals per meter squared (similar to stocking number). Influences canopy height and biomass heat storage.		Canopy height / biomass heat storage	0.03	0.035 to 100^a	0.5	number/m^2	Expert judgment	

Table S5: Land parameters used in this study.

[a]Parameter ranges vary depending on the plant functional type.